Carbon dioxide sequestration on fly ash/waste glassalkali-based mortars with recycled aggregates: compressive strength, hydration products, carbon footprint, and cost analysis

13

Mohammad Mastali [1], *Zahra Abdollahnejad* [1], *Fernando Pacheco-Torgal* [1,2]
[1]University of Minho, Guimarães, Portugal; [2]University of Sungkyunkwan, Suwon, Republic of Korea

13.1 Introduction

Carbon dioxide sequestration is crucial for limiting global warming (Hansen et al., 2017). That is why carbon sequestration constitutes one of the Grande Challenges of Engineering (Mote et al., 2016). Currently this carbon sequestration is carried out mostly through geologic CO_2 storage in saline aquifers (Zhang and Huisingh, 2017). However, that constitutes a passive strategy, involves huge risks, and also comes with a very high cost. Carbon capture and storage from the stream of concentrated CO_2 at fossil fuel burning sites like power plants or steel plants is more efficient and thus less expensive than direct air capture (Hansen et al., 2017). Several authors (Bertos et al., 2004; Jang et al., 2016) have studied the use of CO_2 for accelerated curing of cementitious construction materials. This technology will in future not only minimize release of carbon dioxide into the atmosphere but also accelerate curing and strength development of those materials. However, so far no studies were performed on alkali-based materials. These materials are produced through the reaction of an aluminosilicate powder (precursor) with an alkaline activator, usually composed by hydroxide, silicate, carbonate, or sulfate leading to the formation of an amorphous aluminosilicate gel and secondary nanocrystalline zeolite-like structures (Provis, 2014). These materials have a particular ability for the reuse of several types of wastes (Payá et al., 2014; Bernal et al., 2016). Some wastes like fly ash (FA) deserve a special attention because they are generated in large amount and have a very low reuse rate. USA has a reuse rate for FA of around 50%, meaning that

Carbon Dioxide Sequestration in Cementitious Construction Materials
https://doi.org/10.1016/B978-0-08-102444-7.00013-7

30 million tons of FA are not reused annually (ACAA, 2016). Waste glass is also a waste that is generated in relevant quantities and that merits increased recycling efforts. In 2010, approximately 425,000 tons of waste glass was produced in Portugal and only 192,000 tons of them were recycled. In Hong Kong, approximately 373 tons of waste glass was generated daily in 2010. The use of waste glass in alkali-activated binders is especially interesting because its high SiO_2 content allows for a reduction in the content of sodium silicate thus reducing the cost of this binder which constitutes one of the shortcomings of alkali-activated materials (Pacheco-Torgal et al., 2016). This justified recent studies on alkali-activated materials containing waste glass (Martinez-Lopez and Escalante-Garcia, 2016; Wang et al., 2016). This chapter presents results of the investigation concerning carbon dioxide sequestration on FA/waste glass alkaline-based mortars with recycled aggregates.

13.2 Experimental program

13.2.1 Materials

The mortars were made of FA, calcium hydroxide, waste glass , ordinary Portland cement (OPC), metakaolin (MK), fine aggregates, recycled aggregates, and a sodium hydroxide solution. The FA was obtained from The PEGO Thermal Power Plant in Portugal and categorized as class B and group N according to the ASTM C618-15. Table 13.1 presents the major oxides of FA particles and MK. The Portland cement is of type I class 42.5R from SECIL; its composition contains 63.3% CaO, 21.4% SiO_2, 4.0% Fe_2O, 3.3% Al_2O_3, 2.4% MgO, and other minor components. The calcium hydroxide was supplied by LUSICAL H100 and contains more than 99% CaO. Waste glass from glass bottles ground for 1 h in a ball mill was also used. The final density of the milled waste glass was 1.27 g/cm^3. Solid sodium hydroxide was supplied by ERCROS, S.A., Spain, and was used to prepare the 8M NaOH solution. Distilled water was used to dissolve the sodium hydroxide flakes to avoid the effect of unknown contaminants in the mixing water. The NaOH mix was made 24 h prior to use in order to have a homogenous solution at room temperature. Three different sand types were used in the mixtures: (1) normal sand; (2) recycled sand; (3) carbonated recycled

Table 13.1 The chemical composition of major oxides of fly ash (FA)

Material	Oxides (wt.%)							
	SiO_2	Al_2O_3	Fe_2O_3	CaO	MgO	Na_2O	K_2O	TiO_2
FA	60.81	22.68	7.64	1.01	2.24	1.45	2.70	1.46

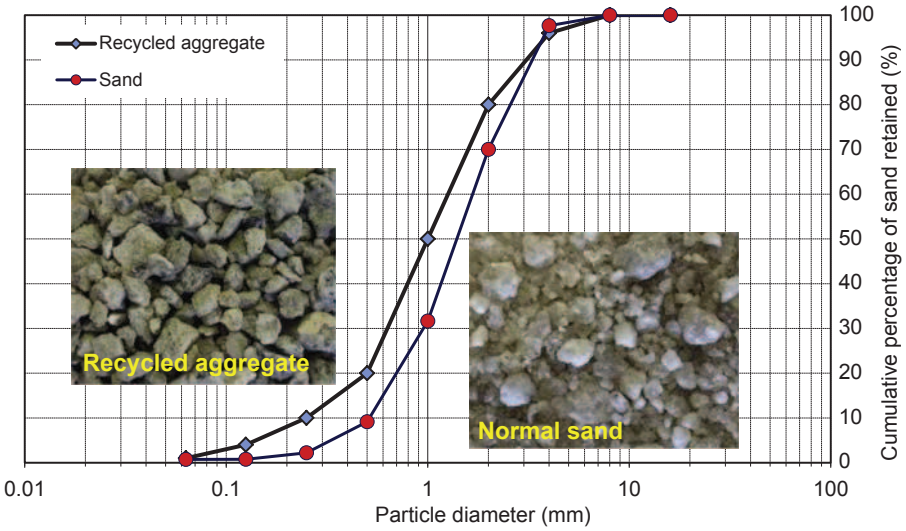

Figure 13.1 Distribution of the sand particles.

aggregate. The normal sand was used as inert filler and was provided from the MIBAL, Minas de Barqueiros, S.A. Portugal. A sieving operation was carried out to remove dust particles. It was dried at 105°C for 24 h, and it was sieved in advance before being used. The dimensions of the sieves were 4.75 and 0.6 mm. The sand had a fineness modulus of 3.885. Recycled sand obtained from the crushing of concrete blocks was also used, after being sieved. The average compressive strength of concrete blocks was around 40 MPa. The detailed grain size distribution of the normal sand and of the recycled sand are presented in Fig. 13.1. The recycled sand has a water absorption of 13%. Recycled sand was carbonated in a carbon chamber from Aralab, model Fitoclima S600 (4.2% CO_2, 40% RH, and 20°C), for 48 h. The recycled sand has a water absorption of 25%. The explanation for the increase of the water absorption relates to the fact that when calcium silicate hydrate (CSH) carbonates its Ca/Si ratio drops and it becomes highly porous. Studies by NMR spectroscopy indicate that decomposition of C-S-H caused by carbonation involves two steps: (1) a gradual decalcification of the C-S-H, where calcium is removed from the interlayer and defect sites in the silicate chains until Ca/Si = 0.67 is reached, ideally corresponding to infinite silicate chains; (2) calcium from the principal layers is consumed, resulting in the final decomposition of the C-S-H and the formation of an amorphous silica phase (Šavija and Luković, 2016).

13.2.2 Mix design and mortar production

Apart from the use of three types of sand, two different sand to binder ratios (4 and 5) were also studied. The composition of the mortars is shown in Table 13.2. In the

Table 13.2 **Mix compositions (kg/m^3)**

Mixtures	Fly ash	CH	PC	MK	MG	SH	Sand	
							Content	Type
80FA_10CH_10MG_NAG	340.0	42.5	–	–	42.5	215.5	1700.0	with normal aggregates, mix cured at lab temp (Sand/Binder: 4)
80FA_10PC_10MG_NAG	341.0	–	43.0	–	43.0	213.0	1706.0	
85FA_5PC_10MG_NAG	362.0	–	43.0	–	43.0	213.0	1705.0	
80FA_10CH_10MK_NAG	345.0	43.0	–	43.0	–	215.7	1725.0	
80FA_10PC_10MK_NAG	347.0	–	43.4	43.4	–	217.0	1735.0	
85FA_5PC_10MK_NAG	368.0	–	21.7	43.4	–	216.7	1733.0	
80FA_5CH_5MK_10MG_NAG	340.0	21.0	–	21.0	42.0	212.0	1698.0	
80FA_5PC_5MK_10MG_NAG	346.6	–	21.6	21.6	21.6	216.0	1733.0	
80FA_10CH_10MG_NAG_CC	340.0	42.5	–	–	42.5	215.5	1700.0	with normal aggregates, mix cured 7 days in carbonation chamber (Sand/Binder: 4)
80FA_10PC_10MG_NAG_CC	341.0	–	43.0	–	43.0	213.0	1706.0	
85FA_5PC_10MG_NAG_CC	362.0	–	43.0	–	43.0	213.0	1705.0	
80FA_10CH_10MK_NAG_CC	345.0	43.0	–	43.0	–	215.7	1725.0	
80FA_10PC_10MK_NAG_CC	347.0	–	43.4	43.4	–	217.0	1735.0	
85FA_5PC_10MK_NAG_CC	368.0	–	21.7	43.4	–	216.7	1733.0	
80FA_5CH_5MK_10MG_NAG_CC	340.0	21.0	–	21.0	42.0	212.0	1698.0	
80FA_5PC_5MK_10MG_NAG_CC	346.6	–	21.6	21.6	21.6	216.0	1733.0	
80FA_10CH_10MG_RAGC	340.0	42.5	–	–	42.5	215.5	1700.0	with recycled carbonated aggregates, mix cured at lab temp (Sand/Binder: 4)
80FA_10PC_10MG_RAGC	341.0	–	43.0	–	43.0	213.0	1706.0	
85FA_5PC_10MG_RAGC	362.0	–	43.0	–	43.0	213.0	1705.0	

80FA_10CH_10MK_RAGC	345.0	43.0	–	43.0	–	215.7	1725.0	
80FA_10PC_10MK_RAGC	347.0	–	43.4	43.4	–	217.0	1735.0	
85FA_5PC_10MK_RAGC	368.0	–	21.7	43.4	–	216.7	1733.0	
80FA_5CH_5MK_10MG_RAGC	340.0	21.0	–	21.0	42.0	212.0	1698.0	
80FA_5PC_5MK_10MG_RAGC	346.6	–	21.6	21.6	21.6	216.0	1733.0	
80FA_10CH_10MG_RAGC_CC	340.0	42.5	–	–	42.5	215.5	1700.0	with recycled carbonated aggregates, mix cured 7 days in carbonation chamber (Sand/Binder: 4)
80FA_10PC_10MG_RAGC_CC	341.0	–	43.0	–	43.0	213.0	1706.0	
85FA_5PC_10MG_RAGC_CC	362.0	–	43.0	–	43.0	213.0	1705.0	
80FA_10CH_10MK_RAGC_CC	345.0	43.0	–	43.0	–	215.7	1725.0	
80FA_10PC_10MK_RAGC_CC	347.0	–	43.4	43.4	–	217.0	1735.0	
85FA_5PC_10MK_RAGC_CC	368.0	–	21.7	43.4	–	216.7	1733.0	
80FA_5CH_5MK_10MG_RAGC_CC	340.0	21.0	–	21.0	42.0	212.0	1698.0	
80FA_5PC_5MK_10MG_RAGC_CC	346.6	–	21.6	21.6	21.6	216.0	1733.0	
80FA_10CH_10MG_RAG	340.0	42.5	–	–	42.5	215.5	1700.0	with recycled aggregates, mix cured at lab temp (Sand/Binder: 4)
80FA_10PC_10MG_RAG	341.0	–	43.0	–	43.0	213.0	1706.0	
85FA_5PC_10MG_RAG	362.0	–	43.0	–	43.0	213.0	1705.0	
80FA_10CH_10MK_RAG	345.0	43.0	–	43.0	–	215.7	1725.0	
80FA_10PC_10MK_RAG	347.0	–	43.4	43.4	–	217.0	1735.0	
85FA_5PC_10MK_RAG	368.0	–	21.7	43.4	–	216.7	1733.0	
80FA_5CH_5MK_10MG_RAG	340.0	21.0	–	21.0	42.0	212.0	1698.0	
80FA_5PC_5MK_10MG_RAG	346.6	–	21.6	21.6	21.6	216.0	1733.0	

Continued

Table 13.2 Continued

Mixtures	Fly ash	CH	PC	MK	MG	SH	Sand	
							Content	Type
80FA_10CH_10MG_RAG_CC	340.0	42.5	–	–	42.5	215.5	1700.0	with recycled aggregates, mix cured 7 days in carbonation chamber (Sand/Binder: 4)
80FA_10PC_10MG_RAG_CC	341.0	–	43.0	–	43.0	213.0	1706.0	
85FA_5PC_10MG_RAG_CC	362.0	–	43.0	–	43.0	213.0	1705.0	
80FA_10CH_10MK_RAG_CC	345.0	43.0	–	43.0	–	215.7	1725.0	
80FA_10PC_10MK_RAG_CC	347.0	–	43.4	43.4	–	217.0	1735.0	
85FA_5PC_10MK_RAG_CC	368.0	–	21.7	43.4	–	216.7	1733.0	
80FA_5CH_5MK_10MG_RAG_CC	340.0	21.0	–	21.0	42.0	212.0	1698.0	
80FA_5PC_5MK_10MG_RAG_CC	346.6	–	21.6	21.6	21.6	216.0	1733.0	
80FA_10CH_10MG_NAG	292.8	36.6	–	–	36.6	183.0	1830.0	with normal aggregates, mix cured at lab temp (Sand/Binder: 5)
80FA_10PC_10MG_NAG	249.4	–	36.8	–	36.8	161.5	1840.0	
85FA_5PC_10MG_NAG	311.9	–	18.3	–	36.7	183.4	1835.0	
80FA_10CH_10MK_NAG	296.0	37.1	–	37.1	–	185.1	1855.0	
80FA_10PC_10MK_NAG	298.4	–	37.3	37.3	–	186.5	1865.0	
85FA_5PC_10MK_NAG	316.5	–	18.6	37.3	–	186.2	1862.5	
80FA_5CH_5MK_10MG_NAG	292.8	18.3	–	18.3	36.6	183.0	1830.0	
80FA_5PC_5MK_10MG_NAG	293.6	–	18.3	18.3	36.6	183.4	1835.0	
80FA_10CH_10MG_NAG_CC	292.8	36.6	–	–	36.6	183.0	1830.0	with normal aggregates, mix cured 7 days in carbonation chamber (Sand/Binder: 5)
80FA_10PC_10MG_NAG_CC	249.4	–	36.8	–	36.8	161.5	1840.0	
85FA_5PC_10MG_NAG_CC	311.9	–	18.3	–	36.7	183.4	1835.0	

80FA_10CH_10MK_NAG_CC	296.0	37.1	–	37.1	–	185.1	1855.0	
80FA_10PC_10MK_NAG_CC	298.4	–	37.3	37.3	–	186.5	1865.0	
85FA_5PC_10MK_NAG_CC	316.5	–	18.6	37.3	–	186.2	1862.5	
80FA_5CH_5MK_10MG_NAG_CC	292.8	18.3	–	18.3	36.6	183.0	1830.0	
80FA_5PC_5MK_10MG_NAG_CC	293.6	–	18.3	18.3	36.6	183.4	1835.0	
80FA_10CH_10MG_RAGC	292.8	36.6	–	–	36.6	183.0	1830.0	with recycled carbonated aggregates, mix cured at lab temp (Sand/Binder: 5)
80FA_10PC_10MG_RAGC	249.4	–	36.8	–	36.8	161.5	1840.0	
85FA_5PC_10MG_RAGC	311.9	–	18.3	–	36.7	183.4	1835.0	
80FA_10CH_10MK_RAGC	296.0	37.1	–	37.1	–	185.1	1855.0	
80FA_10PC_10MK_RAGC	298.4	–	37.3	37.3	–	186.5	1865.0	
85FA_5PC_10MK_RAGC	316.5	–	18.6	37.3	–	186.2	1862.5	
80FA_5CH_5MK_10MG_RAGC	292.8	18.3	–	18.3	36.6	183.0	1830.0	
80FA_5PC_5MK_10MG_RAGC	293.6	–	18.3	18.3	36.6	183.4	1835.0	
80FA_10CH_10MG_RAGC_CC	292.8	36.6	–	–	36.6	183.0	1830.0	with recycled carbonated aggregates, mix cured 7 days in carbonation chamber (Sand/Binder: 5)
80FA_10PC_10MG_RAGC_CC	249.4	–	36.8	–	36.8	161.5	1840.0	
85FA_5PC_10MG_RAGC_CC	311.9	–	18.3	–	36.7	183.4	1835.0	
80FA_10CH_10MK_RAGC_CC	296.0	37.1	–	37.1	–	185.1	1855.0	
80FA_10PC_10MK_RAGC_CC	298.4	–	37.3	37.3	–	186.5	1865.0	
85FA_5PC_10MK_RAGC_CC	316.5	–	18.6	37.3	–	186.2	1862.5	
80FA_5CH_5MK_10MG_RAGC_CC	292.8	18.3	–	18.3	36.6	183.0	1830.0	
80FA_5PC_5MK_10MG_RAGC_CC	293.6	–	18.3	18.3	36.6	183.4	1835.0	

Continued

Table 13.2 Continued

Mixtures	Fly ash	CH	PC	MK	MG	SH	Sand	
							Content	Type
80FA_10CH_10MG_RAG	292.8	36.6	–	–	36.6	183.0	1830.0	with recycled aggregates, mix cured at lab temp (Sand/Binder: 5)
80FA_10PC_10MG_RAG	249.4	–	36.8	–	36.8	161.5	1840.0	
85FA_5PC_10MG_RAG	311.9	–	18.3	–	36.7	183.4	1835.0	
80FA_10CH_10MK_RAG	296.0	37.1	–	37.1	–	185.1	1855.0	
80FA_10PC_10MK_RAG	298.4	–	37.3	37.3	–	186.5	1865.0	
85FA_5PC_10MK_RAG	316.5	–	18.6	37.3	–	186.2	1862.5	
80FA_5CH_5MK_10MG_RAG	292.8	18.3	–	18.3	36.6	183.0	1830.0	
80FA_5PC_5MK_10MG_RAG	293.6	–	18.3	18.3	36.6	183.4	1835.0	
80FA_10CH_10MG_RAG_CC	292.8	36.6	–	–	36.6	183.0	1830.0	with recycled aggregates, mix cured 7 days in carbonation chamber (Sand/Binder: 5)
80FA_10PC_10MG_RAG_CC	249.4	–	36.8	–	36.8	161.5	1840.0	
85FA_5PC_10MG_RAG_CC	311.9	–	18.3	–	36.7	183.4	1835.0	
80FA_10CH_10MK_RAG_CC	296.0	37.1	–	37.1	–	185.1	1855.0	
80FA_10PC_10MK_RAG_CC	298.4	–	37.3	37.3	–	186.5	1865.0	
85FA_5PC_10MK_RAG_CC	316.5	–	18.6	37.3	–	186.2	1862.5	
80FA_5CH_5MK_10MG_RAG_CC	292.8	18.3	–	18.3	36.6	183.0	1830.0	
80FA_5PC_5MK_10MG_RAG_CC	293.6	–	18.3	18.3	36.6	183.4	1835.0	

batching process of the mortars, dry ingredients [FA, sand, calcium hydroxide (or cement), MK, and milled glass] were mixed for 2 min. Then, sodium hydroxide was added and again mixed for 5 min. Then, the mixed mortars were cast into cubic molds ($50 \times 50 \times 50$ mm^3) to assess the compressive strength of different mix compositions. The specimens were cured for 24 h in lab conditions (averagely 25°C and 40% RH) and then they were demolded. Two different curing regimes were used, including: (1) curing at the ambient temperature of lab (average temperature of 25°C and 40% RH); (2) curing in the carbonation chamber (4.2% CO_2 concentration and 40% RH) for 7 days and curing in lab conditions for the remaining days. The preliminary experiments showed that all mixtures were fully carbonated for 7 days through a CO_2 preconditioning curing. Two hundred and eighty-eight cubic specimens with dimension of $50 \times 50 \times 50$ mm^3 were cast and used to measure the CO_2 sequestration in different mixtures by using a furnace decomposition method (Shao and El-hassan, 2016). For each mixture, three specimens were tested and the average was presented as the absorbed CO_2. The carbonated specimens were placed initially in the oven at 105°C for 24 h to evaporate any absorbed water. Then, the weights of the dried specimens were recorded. Afterwards, the specimens were put in the calciner at a temperature between 500 and 850°C for 4 h to measure the water bound to hydration products and carbon dioxide in carbonates. The results revealed that 800°C could be used as the appropriate decomposition temperature.

13.2.3 Test procedures

13.2.3.1 Compressive strength

The compressive strengths of the mixtures were assessed at 7, 14, and 28 days. The compressive strength of each mixture was obtained by averaging the replicated three cubes. All cubic specimens were assessed under compressive load with a constant displacement rate of 0.30 N/mm^2. based on the ASTM C109 recommendation. The compressive load was measured with a load cell of 200 kN capacity.

13.2.3.2 Microstructural analysis

Small samples with 1 cm diameter and 1 cm height were extracted for scanning electron microscopy-energy dispersive spectroscopy (SEM/EDS) testing. The microstructural observation for different geopolymer mortar mixtures was carried out using standard SEM/EDS microscopy (NOVA 200 Nano SEM). Micrographs and chemical compositions were collected at accelerated voltage of 10 and 15 kV, respectively, and variable working distance from 6 to 8 mm. The cylindrical sub-samples from zones 1 to 3 were coated with a 30-nm thick layer of gold-Palladium (60% gold and 40% palladium) alloy; then the SEM/EDS examination for all the specimens were conducted.

13.2.3.3 Fourier transform infrared spectroscopy

The specimens resulting from SEM/EDS tests were also tested by Fourier Transform Infrared Spectroscopy (FTIR). The analysis of infrared transmission spectra was carried out through attenuated total reflectance mode (ATR), using a Perkin Elmer FTIR Spectrum BX with an ATR. PIKE MIRacle Specimens for FTIR study were prepared by mixing 1 mg of sample in 100 mg of KBr as suggested by Zhang et al. (1996). The IR spectra were recorded over a range of 4000 and 400 cm^{-1} at resolution 4 cm^{-1}.

13.3 Results and discussion

13.3.1 Compressive strength

The effects of using different sand types and contents, and different curing regimes on the compressive strengths of the mixtures are shown in Figs. 13.2–13.7. Figs. 13.2–13.4 are related to a sand to binder ratio of 4 while the compressive strength results of mixtures with a sand to binder ratio of 5 are depicted in Figs. 13.5–13.7. Fig. 13.2 shows the compressive strengths of the mixtures containing normal sand. It was observed that using simultaneously equal content of Portland cement and MK had the highest impact on increasing the compressive strength. Mixtures based on waste glass show low compressive strength results. Other authors (Redden and Neithalath, 2014) showed that silica in the glass powder reacts with the alkalis forming sodium silicate gel which is not as dense as CSH gel. Results show that replacing calcium hydroxide by Portland cement increased the compressive strength. Portland cement being a reactive pozzolan leads to the formation of a higher amount of CSH gel. This is because of the low sodium hydroxide concentration used in the present study (Garcia-Lodeiro et al., 2016). In general, it was observed that mixtures exposed to accelerated carbonation curing showed increased compressive strength. The maximum increase of the compressive strength for the mixtures cured by accelerated CO_2 curing as compared to the mixtures cured at the ambient temperature was recorded in the mixture of 80FA_5PC_5MK_10WG_-NAG, so that this increase at ages of 7, 14, and 28 days were about 22 times (4.08 MPa), 6 times (6 MPa), and 5 times (7 MPa), respectively. Afterwards, the maximum compressive strength was recorded for the mixture of 80FA_10PC_10MK_NAG. Curing specimens under a flow-through CO_2 gas increased two and three times the compressive strength of specimens at the ages of 7 and 28 days, respectively. The carbonation of alkali-activated materials is a chemically controlled mechanism that occurs in two steps: (1) carbonation of the pore solution leading to a reduction in pH and the eventual precipitation of Na-rich carbonates, followed by (2) the decalcification of Ca-rich phases (mainly C-S-H, as portlandite usually does not form in these systems) and carbonation of secondary reaction products present in the system (Bernal, 2014). Kwasny et al. (2014) also noticed that using accelerated CO_2 curing increases the rate of the initial hydration of the carbonated cementitious pastes. This increase in

compressive strength can be related to the fact that carbonation curing refines the porosity and pore size of the cementitious pastes as reported by others (He et al., 2016; Jang and Lee, 2016). Fig. 13.3 depicts the effects of using recycled aggregates on the compressive strength. No consistent trend was detected for the compressive strength. For the tested specimens at age of 7 days, using CO_2-curing resulted in measuring the maximum increase of the compressive strength (more than 5 times

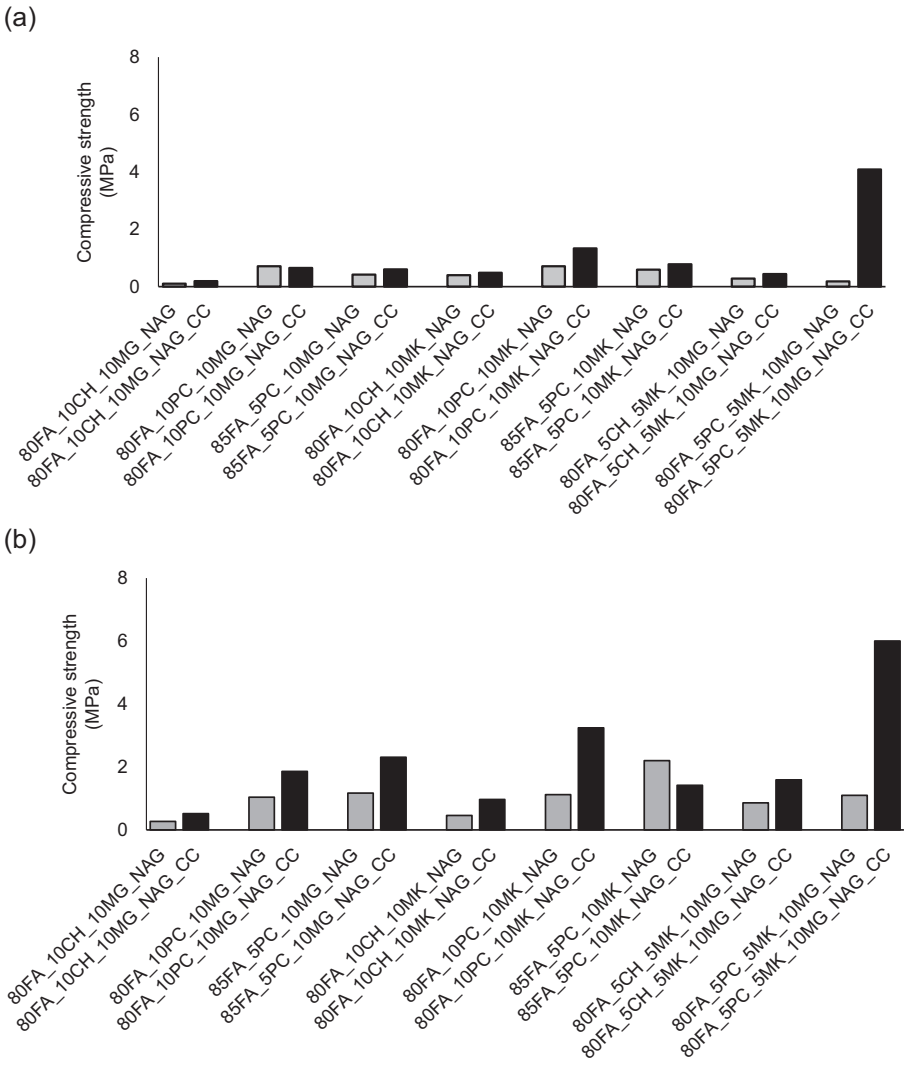

Figure 13.2 Effect of using normal sand with sand to binder ratio of 4 and different curing regimes on the compressive strength at age of: (a) 7 days; (b) 14 days; (c) 28 days.

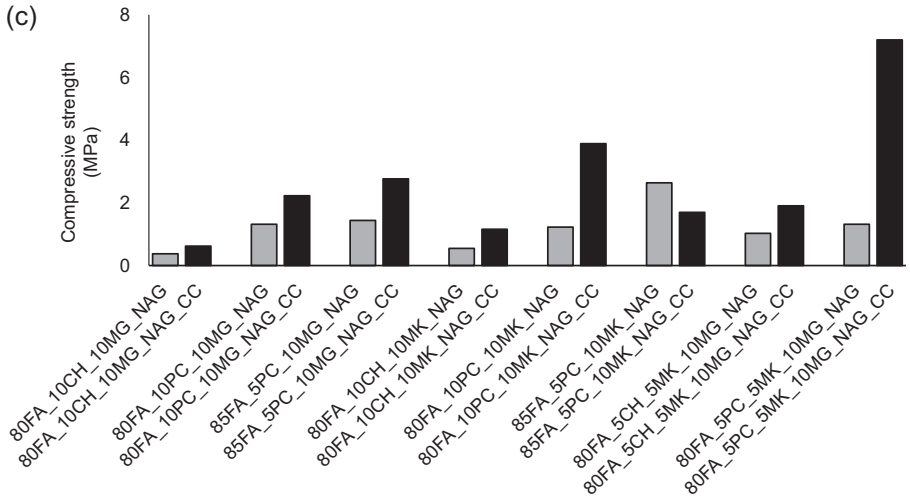

Figure 13.2 cont'd.

(2.73 MPa)) in the mixture of 80FA_10CH_10MG_RAG, as compared with the cured specimens at the ambient temperature. Employing this curing method reduced about 40% the compressive strength of 80FA_5PC_5MK_10MG_RAG, when compared to the cured specimens at the ambient temperature. The effects of using carbonated recycled aggregates on the compressive strength of different mixtures are depicted in Fig. 13.4. It is noticed that the compressive strength increased for all mixtures. Regardless of the duration of curing, the maximum increase of the compressive strength after 7 days curing was recorded for the mixture of 80FA_10CH_10MG_RAGC of around 7 MPa. Moreover, it was observed that by increasing the curing time, an increase in compressive strength is noticed. Using accelerated CO_2 curing increased about 9, 5, and 2 times the compressive strength, when compared to the compressive strength of specimens cured at the ambient temperature. In addition, it was also noticed that using carbonated recycled aggregates significantly increased the compressive strength when compared to using normal sand or recycled aggregate. The maximum compressive strength obtained was about 15 MPa in the mixture 80FA_10CH_10MK_RAGC_CC, cured for 28 days. The effect of using normal sand on the compressive strength of the mixtures is depicted in Fig. 13.5. The use of accelerated CO_2 curing shows no consistent trend on the compressive strength of the mixtures at an early age (7 days), so the maximum increase and decrease of the compressive strength of mixtures due to using of flow-through CO_2-curing at early age were measured in the mixtures of 85FA_5PC_10MG_NAG (with 2.5 times increase) and 80FA_10PC_10MK_NAG (with 40% reduction), respectively. With

respect to the results shown in Fig. 13.5(b) and (c), the maximum increase in the compressive strength was recorded in the mixture 80FA_5PC_5MK_10MG_NAG (more than 2 times for both 14 and 28 days). Afterwards, the maximum increase of the compressive strength was measured for the mixture 80FA_10PC_10MG_NAG

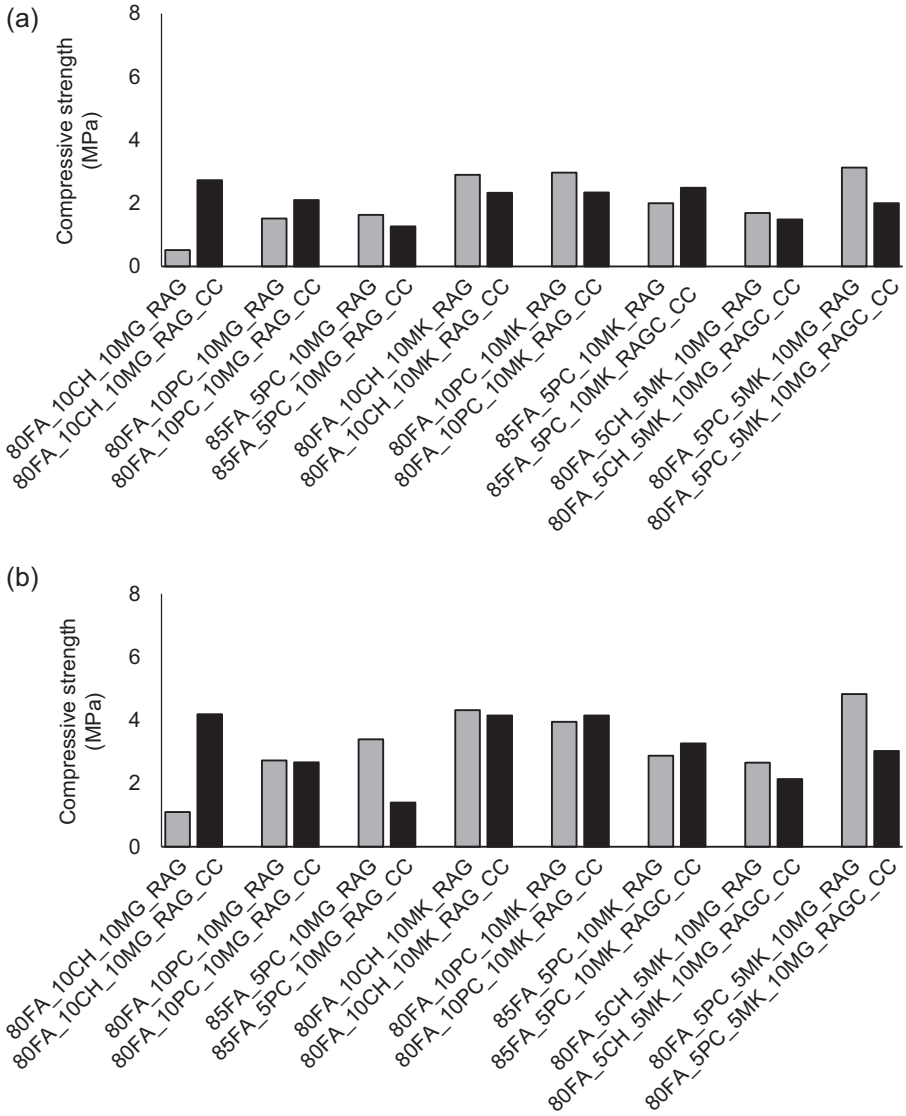

Figure 13.3 Effect of using recycled sand with sand to binder ratio of 4 and different curing regimes on the compressive strength of: (a) 7 days; (b) 14 days; (c) 28 days.

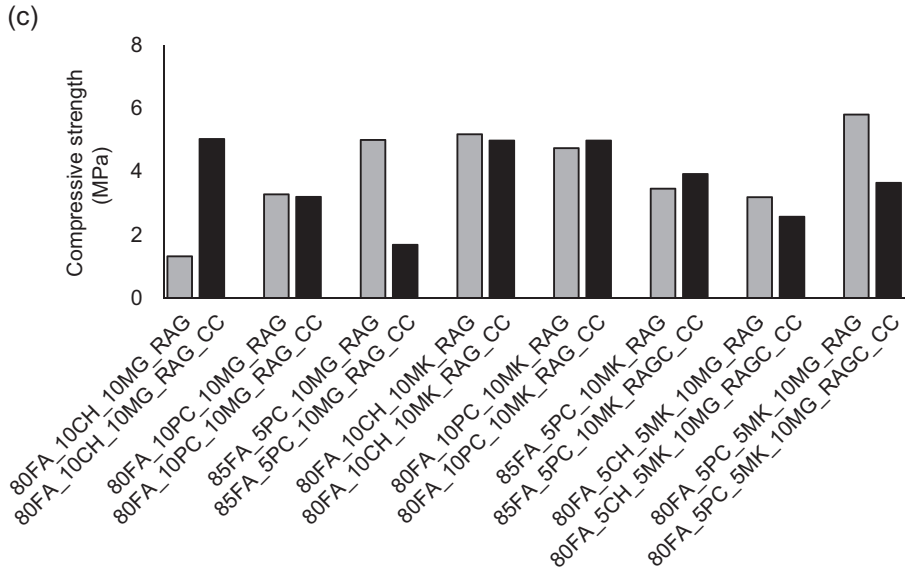

Figure 13.3 cont'd.

(about 2 times for both 14 and 28 days). Generally, comparing Figs. 13.2 and 13.5 indicates that increasing the content of normal sand to binder ratio from 1:4 to 1:5 reduced the efficiency of accelerated CO_2 curing, which may be due to an increase in the pore content. Also a reduction of the tortuosity of the cracking path may have taken place. A shorter tortuous crack path decreases the ultimate energy absorption capacity reached to the failure and subsequently decreases the compressive strength (Larrard and Belloc, 1997). Fig. 13.6 shows the compressive strengths of mixtures containing recycled aggregates to binder in the ratio of 5. Regardless of the curing time, a consistent trend on increasing or decreasing the compressive strength of mixtures was not noticed due to the use of accelerated CO_2 curing method, so that the maximum decrease and increase of the compressive strength at 7 days were recorded to be 55% and 3.5 times for the mixtures of 80FA_10CH_10MK_-RAG and 80FA_5PC_5MK_10MG_RAGC, respectively, as compared to curing the specimens at ambient temperature. The maximum decrease and increase of the compressive strength at 14 and 28 days were recorded to be about 50% and 2.5 times for the mixtures of 85FA_5PC_10MG_RAG and 80FA_5PC_5MK_10MG_RAGC, respectively. Fig. 13.7 shows the influence of increasing the content of carbonated recycled aggregates. The results show that increasing carbonated recycled aggregates significantly affected and increased the compressive strength of mixtures. Due to accelerated CO_2-curing, the maximum increase of the compressive strength

compared to cured specimens at the ambient temperature was recorded in the mixture 80FA_10CH_10MG_RAGC, and it was observed that the compressive strength increased more than 5 times at early age (7 days) and 4 times for specimen at age of 14 and 28 days. Moreover, by increasing the sand to binder ratio from 4 to 5, a

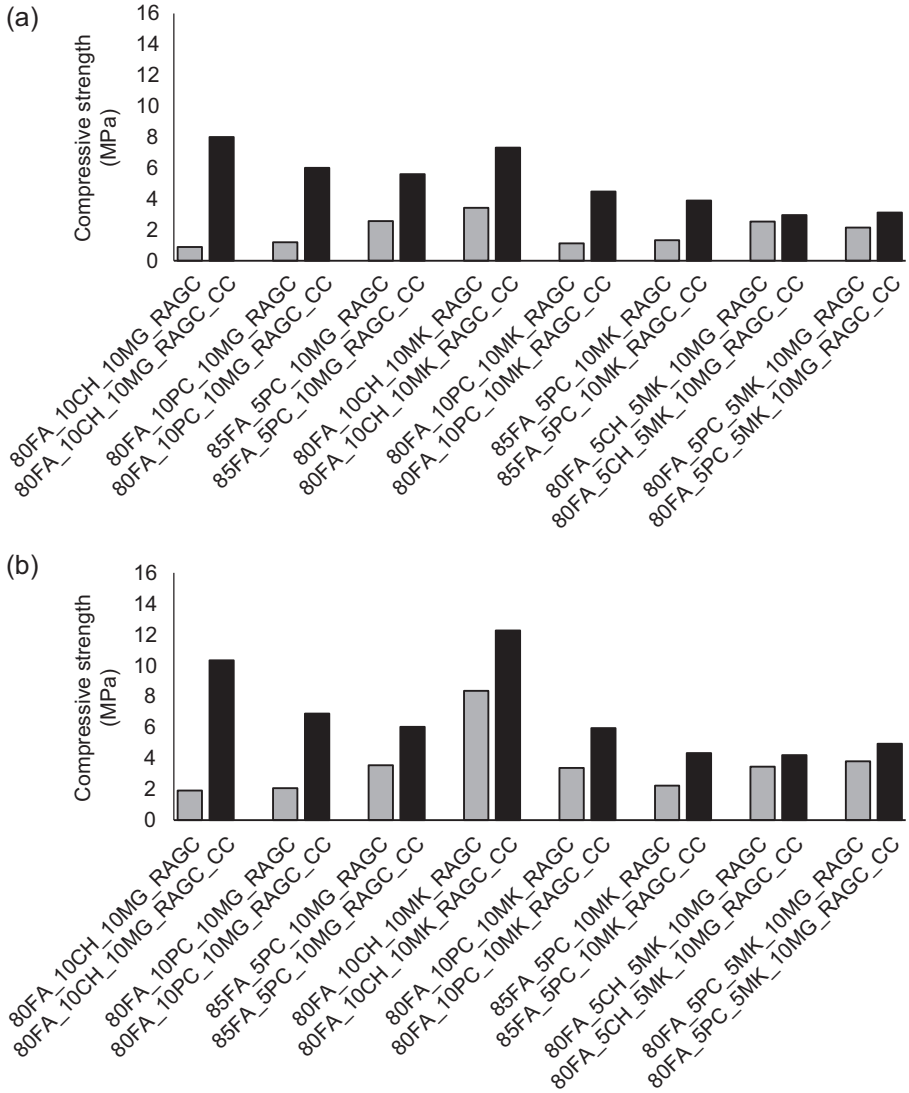

Figure 13.4 Effect of using carbonated recycled sand with sand to binder ratio of 4 and different curing regimes on the compressive strength of: (a) 7 days; (b) 14 days; (c) 28 days.

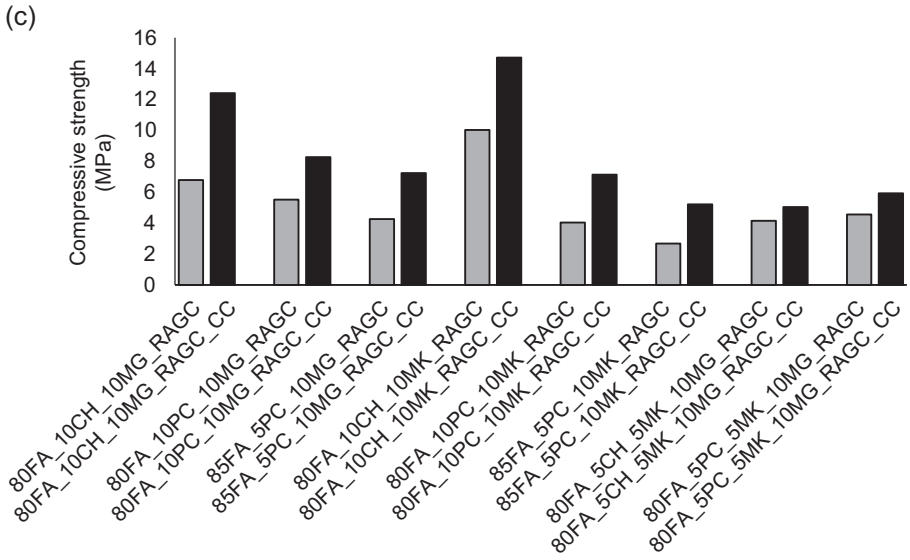

Figure 13.4 cont'd.

maximum compressive strength equal to 10.1 MPa was measured in the mixture 80FA_10CH_10MG_RAGC_CC, which was cured for 28 days.

13.3.2 Microstructural analysis and fourier transform infrared spectroscopy

Fig. 13.8 shows the SEM/EDS analysis of the mixtures 80FA_10CH_10MG_NAG (compressive strength 0.62 MPa), 80FA_10CH_10MG_NAG_CC (5.03 MPa), and 80FA_10CH_10MG_RAGC_CC (12.41 MPa). The results show that accelerated CO_2 curing led to a high formation of calcium carbonate ($Ca(CO)_3$) from the carbonation of calcium hydroxide, calcium-silicate-hydrate (CSH) (tobermorite), and even unhydrated constituents (Peter et al., 2008). Vaterite (PDF#33-0268) was also detected as a metastable polymorph which readily transformed into the stable phase—calcite (Han et al., 2005). After carbonation, the soluble sodium ion content decreased dramatically and the soluble sodium ions solidification ratio was dependent on the content of vaterite formed during the carbonation. Other authors also mention that soluble sodium ions can be solidified in crystalline vaterite by carbonation (Liu et al., 2017). XRD results in Fig. 13.9 show that accelerated CO_2 curing resulted in the reducing of intensity of the sodium peak while increasing the peaks of silica, aluminum, and calcium. Table 13.3 presents EDS atomic ratios. The results show that accelerated CO_2 curing

led to increase in the Al_2O_3/Na_2O and CaO/SiO_2 ratios and a decrease of the Na_2O/CaO and MgO/Al_2O_3 ratios. The C/S ratio is in line with the ones of carbonated calcium silicates reported by Ashraf and Olek (2016). Fig. 13.10 presents the FTIR spectra for the same mixtures. The FTIR spectra for silicate compounds

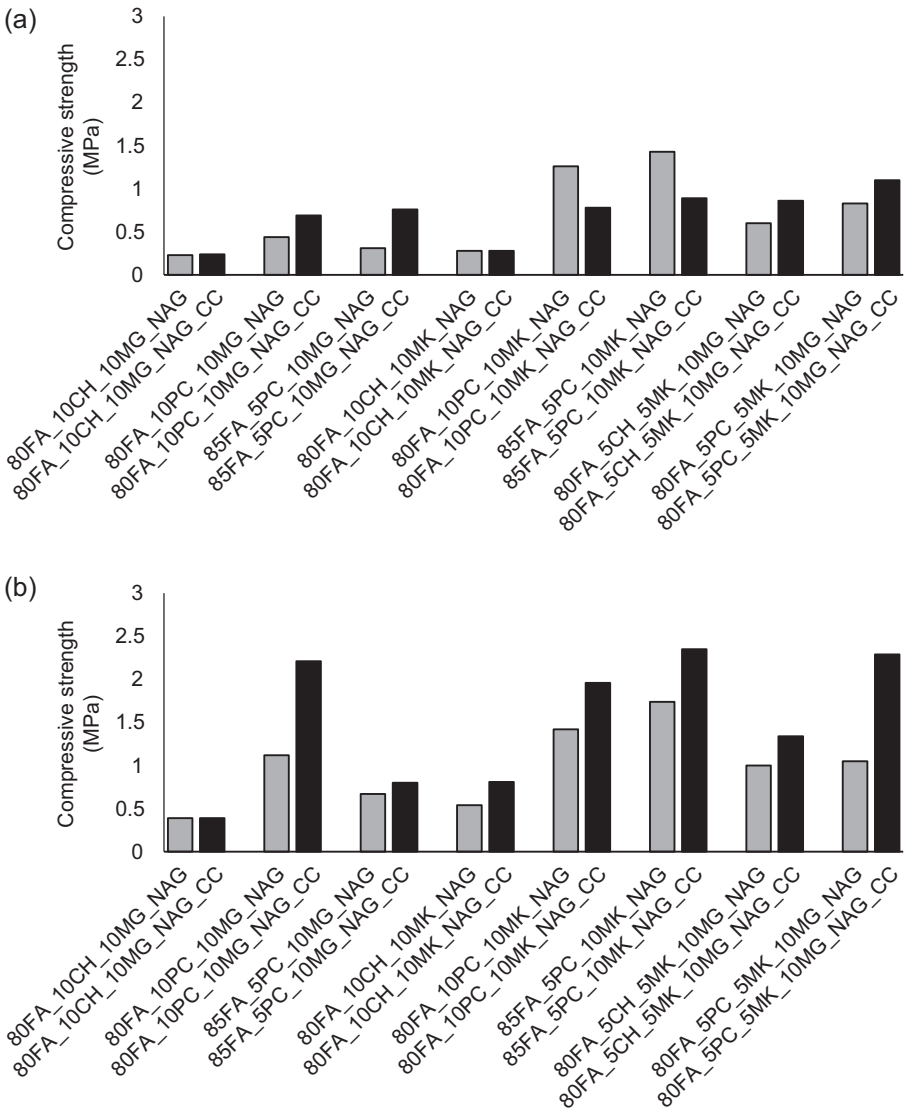

Figure 13.5 Effect of using normal sand with sand to binder ratio of 5 and different curing regimes on the compressive strength of: (a) 7 days; (b) 14 days; (c) 28 days.

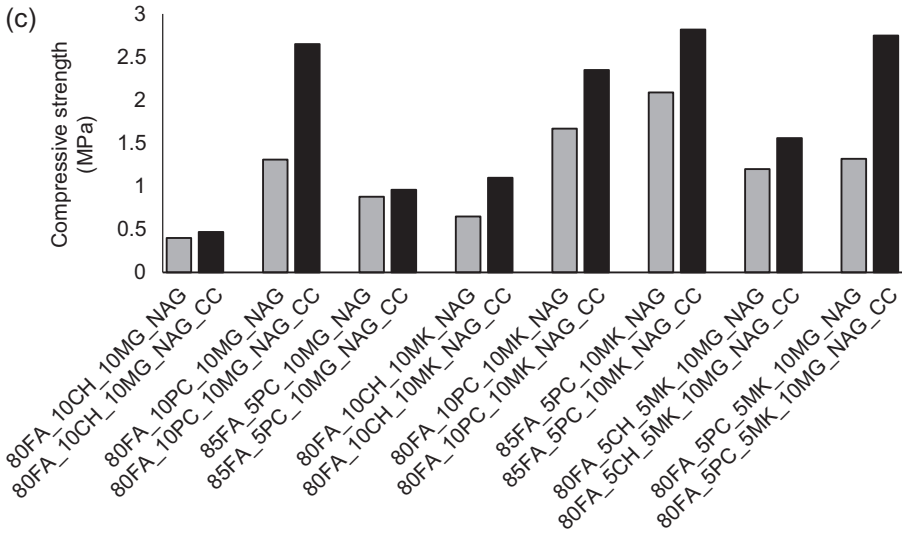

Figure 13.5 cont'd.

exhibits a large absorption between 800 and 1200 cm^{-1} which correspond to the asymmetrical stretching vibration of Si−O bond. The shifts to higher wave number with increasing degree of polymerization of the silicate compound are due to calcium to silica atomic ratio of the calcium-silica gel phase as this ratio also represents the degree of silicate polymerization of the CSH (Yu et al., 1999). Carbonates from calcite vibration occur at 2930−2920 cm^{-1} and 2855−2850 cm^{-1}. Water absorbs infrared radiation between 1600 and 1700 cm^{-1} due to its bending vibration and also in the range 3000−3700 cm^{-1} as this corresponds to the O−H stretching region (Ylmen and Jäglid, 2013). Hydrated minerals, such as portlandite, at 3643 cm^{-1} are noticed.

13.3.3 CO_2 sequestration

Fig. 13.11 shows the effects of increasing the cement content from 5% to 10% in the mixtures containing different sand content and types. Regarding the results in Fig. 13.11(a), except the mixtures containing recycled carbonated aggregate to binder ratio of 5 and milled glass, increasing the cement content increased the CO_2 sequestration. The results also revealed that the maximum increase of the CO_2 sequestration was detected to be about 24 $kgCO_2eq/m^3$ due to increase of cement content from 5% to 10% in the mixtures of 80FA_5PC_10MG_NAG_CC and 80FA_10PC_10MG_NAG_CC. Additionally, no specific trend could be found by increasing the cement content from 5% to 10% in the mixtures containing MK,

as indicated in Fig. 13.11(b). Regardless of the use of milled glass or MK, it was observed that increasing the sand ratio from 4 to 5 reduced the CO_2 sequestration. The experimental results in this chapter indicate that other supplementary cementitious materials, sand content, and type could also contribute to the CO_2 sequestration,

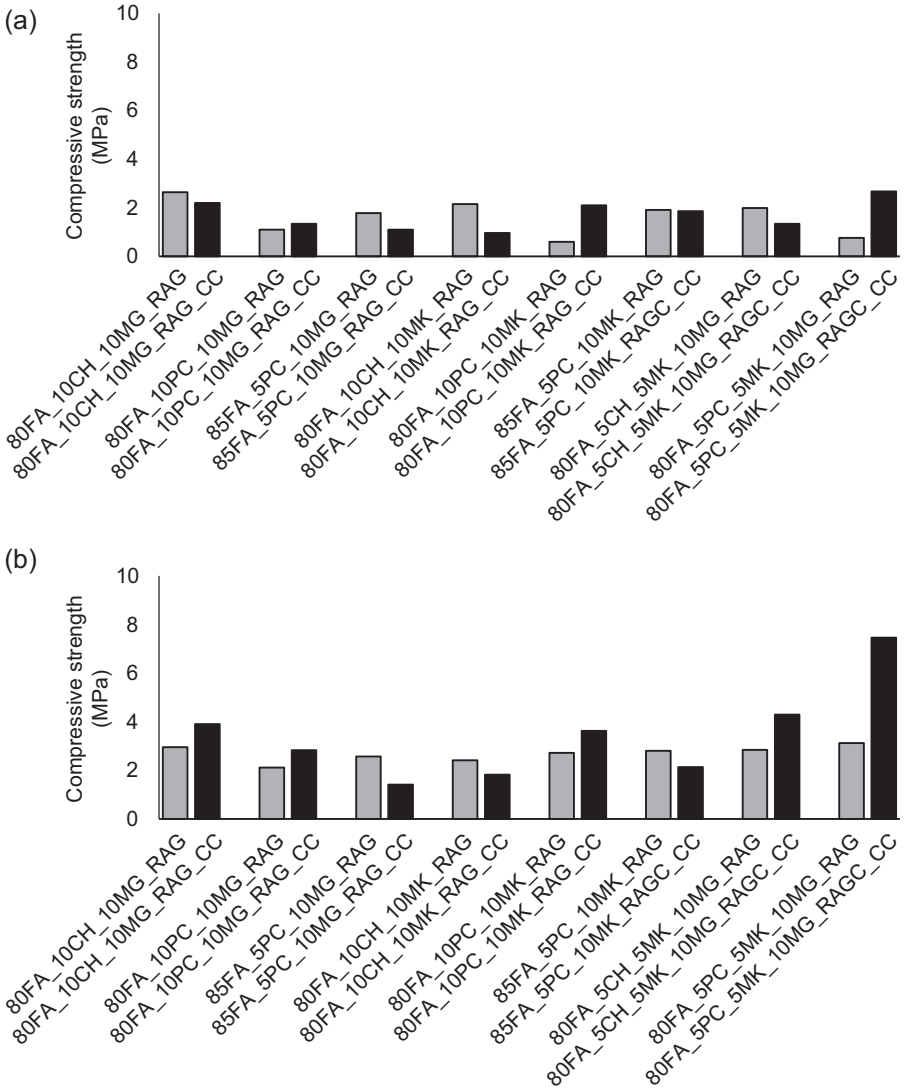

Figure 13.6 Effect of using recycled sand with sand to binder ratio of 5 and different curing regimes on the compressive strength of: (a) 7 days; (b) 14 days; (c) 28 days.

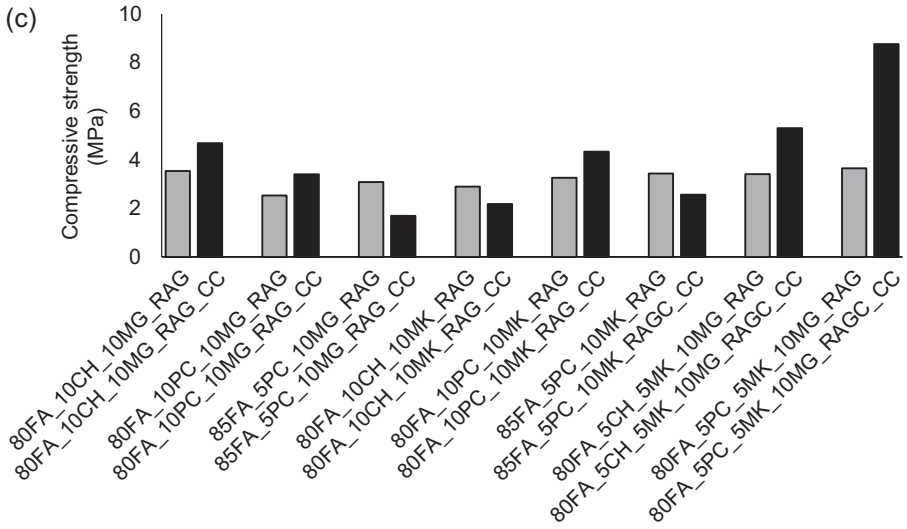

Figure 13.6 cont'd.

and increasing the cement content does not necessarily lead to increase in the CO_2 sequestration. Several authors (Rostami et al., 2011; El-Hassan and Shao, 2014, 2015) have studied the CO_2 sequestration using accelerated CO_2 curing in the concrete blocks containing 13% cement and they reported a sequestration of 75 $kgCO_2eq/m^3$. Thus, regardless the use of milled glass or MK, the CO_2 sequestration in the mixtures containing cement (5% and 10%) was measured in the range of 17−112 $kgCO_2eq/m^3$ in the present study. Effects of replacing cement by calcium hydroxide are depicted in Fig. 13.12. For the mixtures containing sand to binder in the ratio 4 and milled glass, except the mixtures containing carbonated recycled aggregates, replacing cement by calcium hydroxide reduced the CO_2 sequestration. With increasing the sand to binder ratio from 4 to 5, replacing cement by calcium hydroxide only reduced the CO_2 sequestration in the mixture with normal sand. Using calcium hydroxide in the mixtures containing recycled aggregates and carbonated recycled aggregates increased the CO_2 sequestration. In the mixtures containing recycled aggregate or recycled carbonated aggregate, the quantity of calcium hydroxide is increased by C-S-H decalcification in the cement paste. Thus, using calcium hydroxide in the mixtures containing recycled aggregate and recycled carbonated aggregate increased the CO_2 sequestration, as compared to the mixtures using cement. Fig. 13.12(b) indicates the CO_2 sequestration of the mixtures containing both milled glass and MK. Reduction of the cement and calcium hydroxide from 10% to 5% and using 5% MK instead increases in the C-S-H gel. These substitutions affect the hydration products and porosity of the mixtures. Moreover, using recycled carbonated aggregate affects the

hydration products and porosity of the mixtures. Regardless of the sand to binder ratio, except the mixture containing sand to binder ratio 4 and recycled aggregate or recycled carbonated aggregate, using calcium hydroxide instead of cement reduced

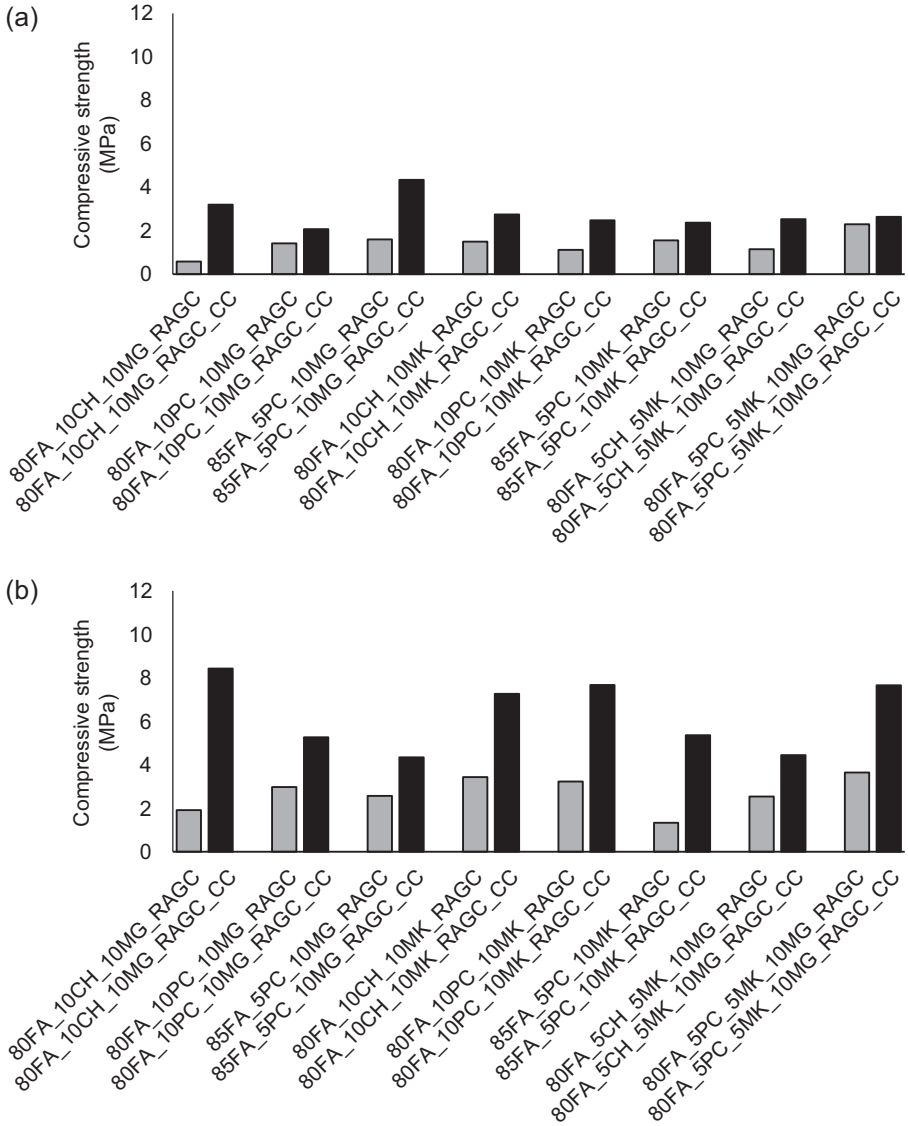

Figure 13.7 Effect of using carbonated recycled sand with sand to binder ratio of 5 and different curing regimes on the compressive strength of: (a) 7 days; (b) 14 days; (c) 28 days.

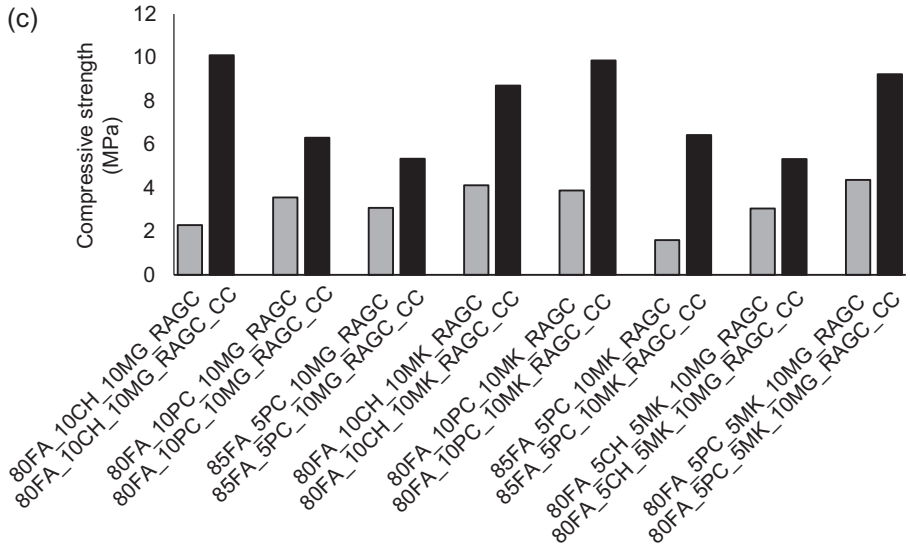

Figure 13.7 cont'd.

the CO_2 sequestration of the mixtures. Since for the mixtures with sand to binder ratio 5, using calcium hydroxide instead of cement reduced the CO_2 sequestration. Fig. 13.13(a) indicates the effects of replacing milled glass by MK in the mixtures containing 10% calcium hydroxide. Regarding the results, using MK instead of milled glass increased the CO_2 sequestration in the mixtures with sand to binder ratio of 4. Increasing the sand to binder ratio from 4 to 5 resulted in no specific trend in the CO_2 sequestration, but replacing milled glass with MK for the mixtures containing recycled aggregate and recycled carbonated aggregate increased the CO_2 sequestration. The results of replacing milled glass with MK in the mixtures containing 10% cement are shown in Fig. 13.13(b). Regardless of the use of sand to binder ratio, except the mixture with normal sand to binder ratio of 4, replacing milled glass with MK reduced the CO_2 sequestration. The maximum effect of replacing milled glass with MK on the CO_2 sequestration was detected in the mixture containing normal sand to binder ratio of 4 (about 25 $kgCO_2eq/m^3$). Fig. 13.13(c) indicates the effects of replacing milled glass by MK in the mixtures containing 5% cement. With respect to the results, using MK in the mixtures with sand to binder ratio 4 increased the CO_2 sequestration, as compared to the mixtures containing milled glass. Except the mixture with normal sand, this trend was also observed for the mixture containing sand to binder ratio of 5. Galan et al. (2010) investigated the effects of different parameters on the CO_2 sequestration of concrete made with OPC. They found the effective parameter on the CO_2 sequestration is the moisture content of

the concrete. In general, concerning the results, it can be concluded that the effects of raw materials on the CO_2 sequestration could be governed by the content and type of both raw materials and sand. Moreover, it was found that the sand to binder ratio and sand type used in the mixtures had the highest impact on increasing or decreasing trend of the CO_2 sequestration in the mixtures. Additionally, regardless of the raw materials and sand to binder ratio, it was observed that using recycled aggregate and recycled carbonated aggregate generally led to maximum CO_2 sequestration in the mixtures.

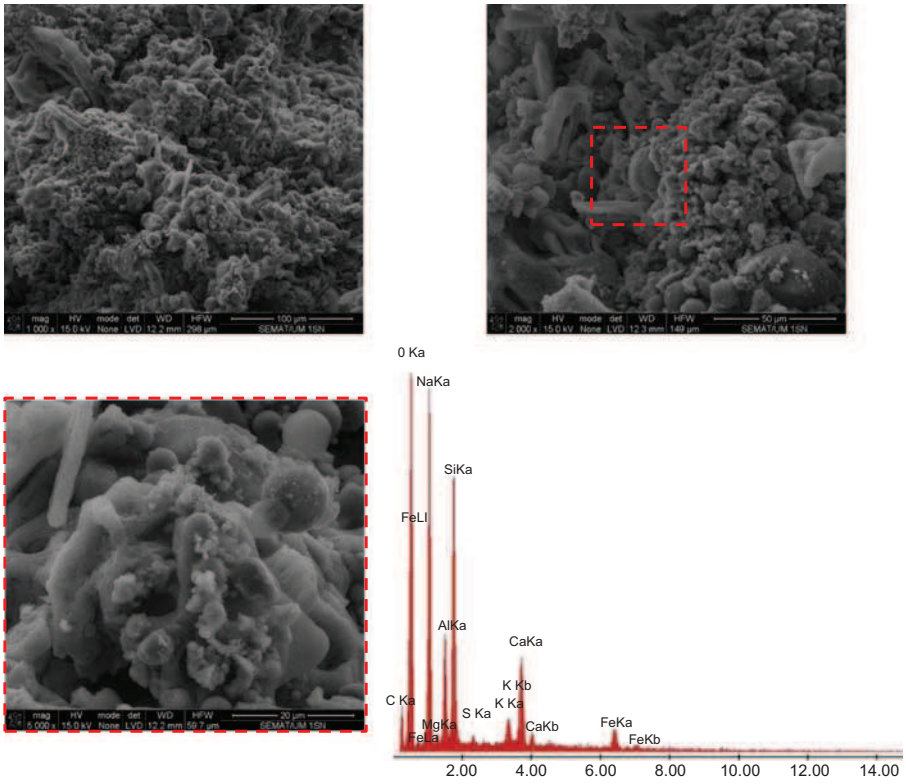

Figure 13.8 SEM/EDS analysis on the mixture 80FA_10CH_10MG containing: (a) Mixture with normal sand and ambient temperature curing; (b) Mixture with normal sand and accelerated CO_2 curing; (c) Mixture with carbonated recycled sand and accelerated CO_2 curing. V-Vaterite, C-Calcite.

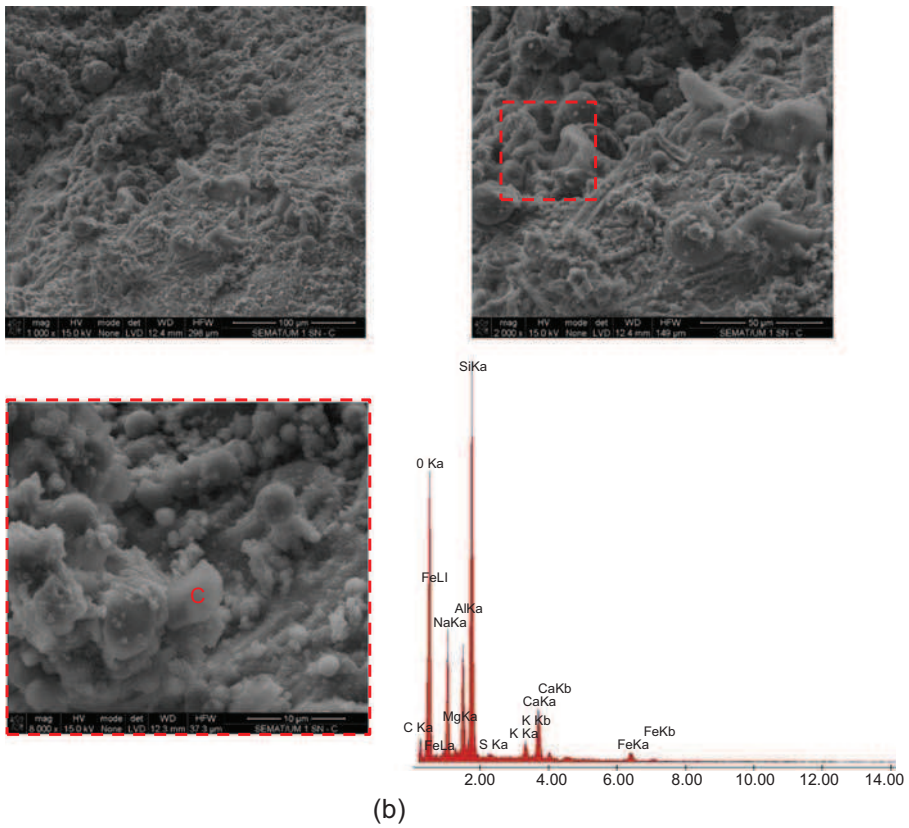

Figure 13.8 cont'd.

13.3.4 Carbon footprint

The carbon footprint ($kgCO_2eq/m^3$) was assessed using the EcoInvent database. Table 13.4 shows the global warming potential for each mortar constituent. The greenhouse gas (GHG) emissions of the mixtures are indicated in Figs. 13.14 and 13.15. Fig. 13.14 shows GHG emissions of different mixtures containing sand to binder ratio 4. Concerning the results, the minimum and maximum CO_2 sequestration for the mixtures containing sand to binder ratio 4 and normal sand were detected to be 80FA_5CH_5MK_10MG_NAG (15 $kgCO_2eq/m^3$) and 80FA_5PC_5MK_10MG_-NAG_CC (61.6 $kgCO_2eq/m^3$). Moreover, the results revealed that using flow-through CO_2 curing reduced the carbon footprint of the mixtures, as compared to the carbon footprint of the specimens cured at ambient temperature regardless of the sand type. The minimum and maximum carbon footprint of the mixtures

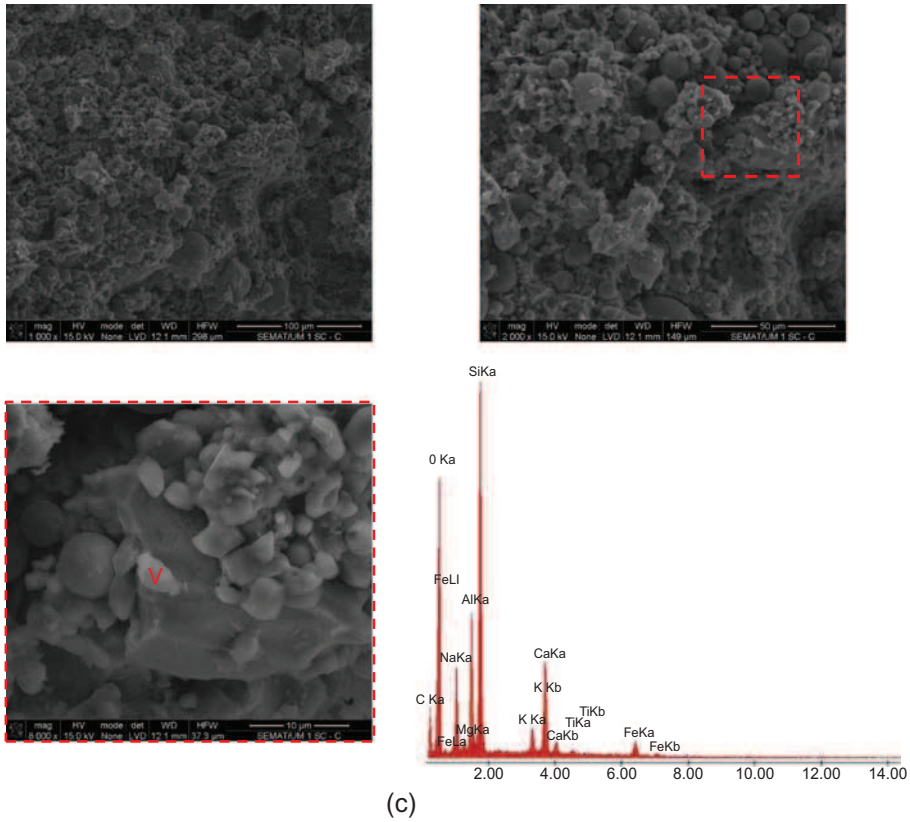

(c)

Figure 13.8 cont'd.

containing sand to binder ratio 4 and normal sand were recorded to be 143.6 and 207.4 $kgCO_2eq/m^3$ in the mixtures 80FA_5PC_5MK_10MG_NAG_CC and 80FA_10PC_10MK_NAG, respectively. As indicated in Fig. 13.14(c) and (d), the minimum and maximum CO_2 sequestration for the mixtures containing sand to binder ratio 4 and recycled aggregate were found to be 85FA_5PC_10MG_RAG (46 $kgCO_2eq/m^3$) and 80FA_10CH_10MK_RAG_CC (113 $kgCO_2eq/m^3$). Thus the minimum and maximum carbon footprint of the mixtures containing sand to binder ratio 4 and recycled aggregate were obtained as 86.4 and 174.7 $kgCO_2eq/m^3$ for the mixtures 80FA_5CH_5MK_10MG_RAG_CC and 85FA_5PC_10MG_RAG, respectively. Regarding the results in Fig. 13.14(e) and (f), the minimum and maximum CO_2 sequestration for the mixtures containing sand to binder ratio 4 and recycled carbonated aggregate were found to be 85FA_5PC_10MG_RAGC (48 $kgCO_2eq/m^3$) and 80FA_10CH_10MK_RAGC_CC (121 $kgCO_2eq/m^3$). Interestingly, it was found that using recycled aggregate and recycled carbonated aggregate had no effect on the mixture

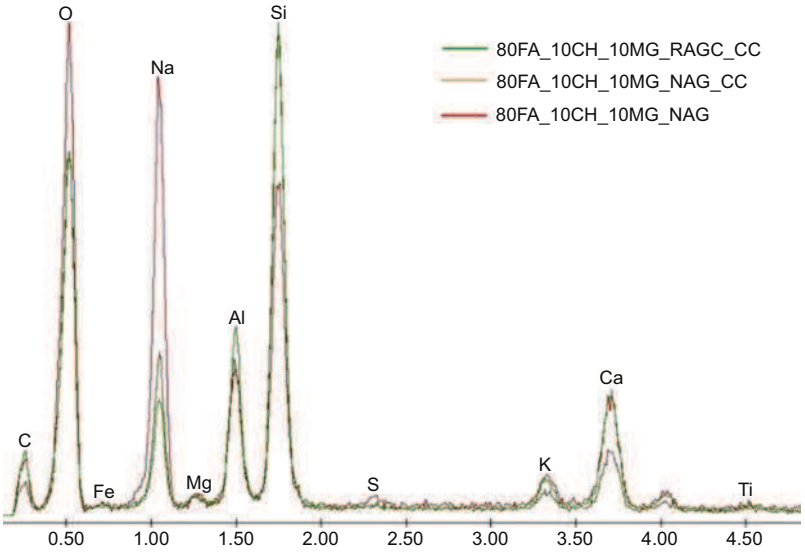

Figure 13.9 XRD of the mixtures 80FA_10CH_10MG_NAG, 80FA_10CH_10MG_NAG_CC, and 80FA_10CH_10MG_RAGC_CC.

Table 13.3 Energy Dispersive Spectroscopy Atomic ratios

Mixture	SiO_2/Al_2O_3	Al_2O_3/Na_2O	CaO/SiO_2	Na_2O/CaO	MgO/Al_2O_3
80FA_10CH_10MG_NAG	4.64	0.22	0.09	10.48	0.20
80FA_10CH_10MG_NAG_CC	6.61	0.60	0.16	6.22	0.18
80FA_10CH_10MG_RAGC_CC	5.48	0.92	0.29	0.67	0.17

ingredients to have the minimum and maximum CO_2 sequestration. Moreover, the minimum and maximum carbon footprint of the mixtures containing sand to binder ratio 4 and recycled carbonated aggregate were measured to be 80.4 and 172.7 $kgCO_2eq/m^3$ for the mixtures 80FA_5CH_5MK_10MG_RAG_CC and 85FA_5PC_10MG_RAG, respectively. Regardless of the sand type, the carbon footprint of the mixtures reduced with increasing the sand content from 4 to 5. With respect to the results gathered, the minimum and maximum CO_2 sequestration for the mixtures containing sand to binder ratio 5 and normal sand were detected 80FA_10CH_10MG_NAG (21 $kgCO_2eq/m^3$) and 80FA_10PC_10MG_NAG_CC (66 $kgCO_2eq/m^3$). Also, it was detected that increasing the sand content from 4 to 5 has impact on the mixture ingredients to

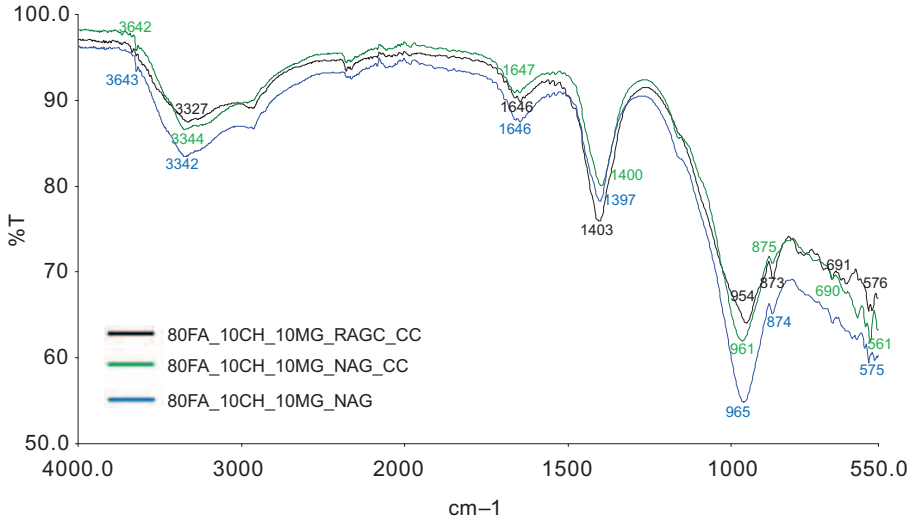

Figure 13.10 Fourier Transform Infrared Spectroscopy spectra for the mixtures 80FA_10CH_10MG_NAG, 80FA_10CH_10MG_NAG_CC, and 80FA_10CH_10MG_RAGC_CC.

have the minimum and maximum CO_2 sequestration. Moreover, it was found that increasing the normal sand content from 4 to 5 increased the minimum and maximum CO_2 sequestration of the mixtures. The minimum and maximum carbon footprint of the mixtures containing sand to binder ratio 5 and normal sand were recorded to be 107 and 165.6 $kgCO_2eq/m^3$ in the mixtures 80FA_10PC_10MG_NAG_CC and 80FA_10PC_10MK_NAG, respectively. For the mixtures with sand to binder ratio 5 and recycled aggregate, the minimum and maximum CO_2 sequestration were obtained in the mixtures of 85FA_5PC_10MG_RAG (30 $kgCO_2eq/m^3$) and 80FA_10CH_10MG_RAG_CC (100 $kgCO_2eq/m^3$), respectively. Additionally, the minimum and maximum carbon footprint attained were 71.9 and 162.6 $kgCO_2eq/m^3$ in the mixtures 80FA_10CH_10MG_RAG_CC and 80FA_10PC_10MK_RAG, respectively. With respect to the results observed in Fig. 13.15(c) and (d), the minimum and maximum CO_2 sequestration in the mixtures containing sand to binder ratio 5 and recycled carbonated aggregate were achieved in the mixtures of 80FA_5CH_5MK_10MG_RAGC (38 $kgCO_2eq/m^3$) and 85FA_5PC_10MK_RAGC_CC (76 $kgCO_2eq/m^3$), respectively. Increasing the content of recycled aggregate and recycled carbonated aggregate from 4 to 5 reduced the minimum and maximum CO_2 sequestration. As shown in Fig. 13.15(e) and (f), the minimum and maximum carbon footprint of the mixtures containing sand to binder ratio 5 and recycled carbonated aggregate were 100.5 and 156.6 $kgCO_2eq/m^3$ in the mixtures 80FA_5PC_5MK_10MG_RAGC_CC and 80FA_10PC_10MK_RAGC, respectively.

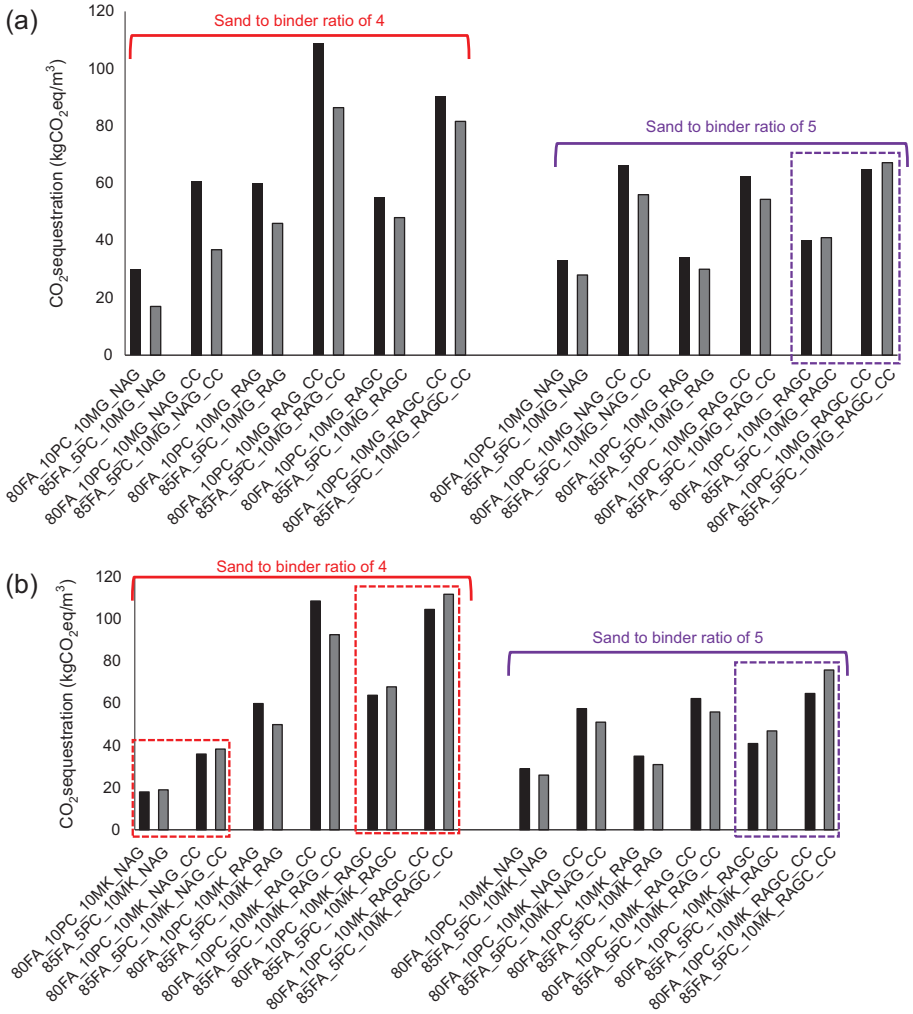

Figure 13.11 Effects of increasing cement content from 5% to 10% on the CO2 sequestration of the mixtures containing: (a) milled glass; (b) metakaolin.

Moreover, regardless of the content and type of the sand used in the mixtures, it was found that using a flow-through CO_2 curing significantly increases the CO_2 sequestration, as compared to the CO_2 sequestration cured at lab temperature. The maximum effect of using a flow-through CO_2 curing on increasing the CO_2 sequestration was found in the mixtures containing normal sand and a sand to binder ratio of 4 (85FA_5PC_10MG_NAG_CC more than 2 times, as compared to 85FA_5PC_10MG_NAG_CC). Ouellet-Plamondon and Habert (2014) reported an embodied carbon of 227 $kgCO_2eq/m^3$

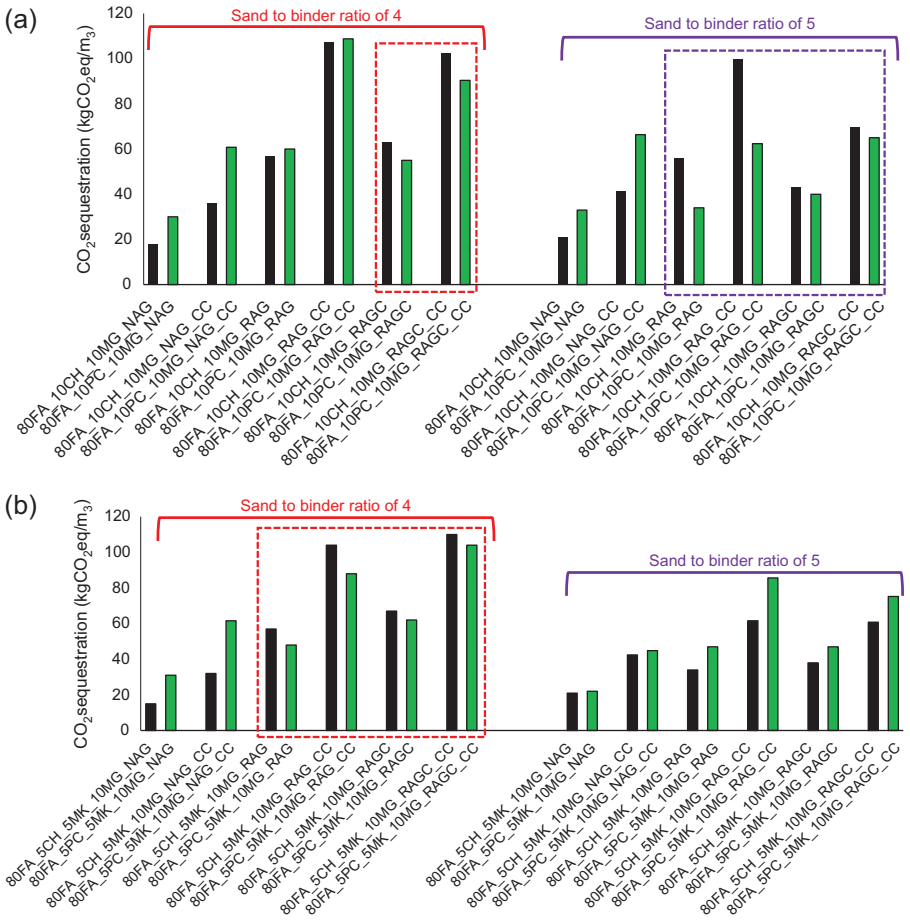

Figure 13.12 Effects of replacing cement by calcium hydroxide on the CO_2 sequestration of the mixtures containing: (a) milled glass; (b) both milled glass and metakaolin.

for a mixture of hybrid cement-based concrete. Also Z. Abdollahnejad et al. (2017) reported global warming potential in range of 178 and 250 $kgCO_2eq/m^3$ for one-part geopolymer foam mortars composed of FA, OPC, calcined kaolin, sodium hydroxide, and $Ca(OH)_2$. Those confirm the very good embodied carbon performance of the mixtures developed in this study.

13.3.5 Correlation between the compressive strength and carbon footprint

Figs. 13.16 and 13.17 depict the normalized carbon footprint to the compressive strength for different mixtures. In general, the use of accelerated CO_2 curing reduced

the normalized carbon footprint to the compressive strength of the mixtures, as compared to the normalized carbon footprint to the compressive strength of the specimens cured at ambient temperature. As indicated in Fig. 13.16(a), the minimum and maximum ratio of the normalized carbon footprint to the compressive strength for the mixtures containing sand to binder ratio 4 and normal sand were found to be 20 and 472.5 $kgCO_2eq/m^3MPa$, for specimens 80FA_5PC_5MK_10MG_NAG_CC and 80FA_10CH_10MG_NAG, respectively. Thus for the mixture with sand to binder ratio 4 and recycled aggregate, the minimum and maximum amount of carbon dioxide released into the atmosphere per 1 MPa were obtained as 18.5 and 108.5 $kgCO_2eq/m^3$

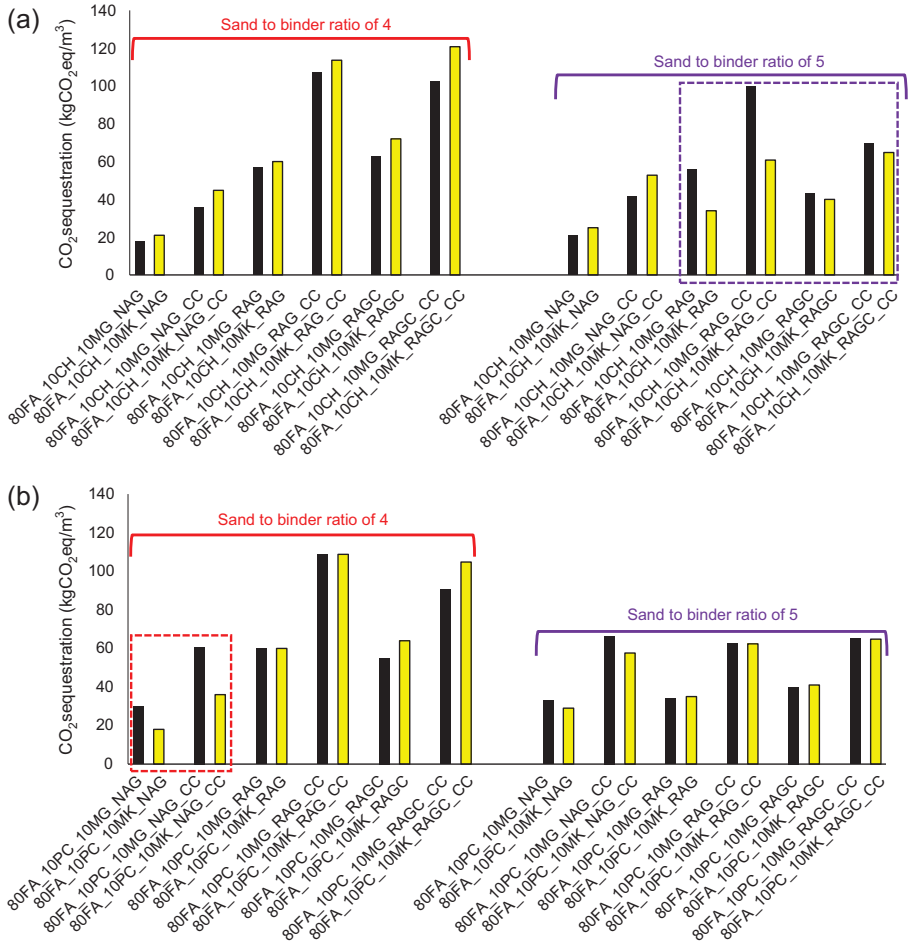

Figure 13.13 Effects of replacing milled glass by calcium metakaolin on the CO_2 sequestration of the mixtures containing: (a) 10% calcium hydroxide; (b) 10% cement; (c) 5% cement.

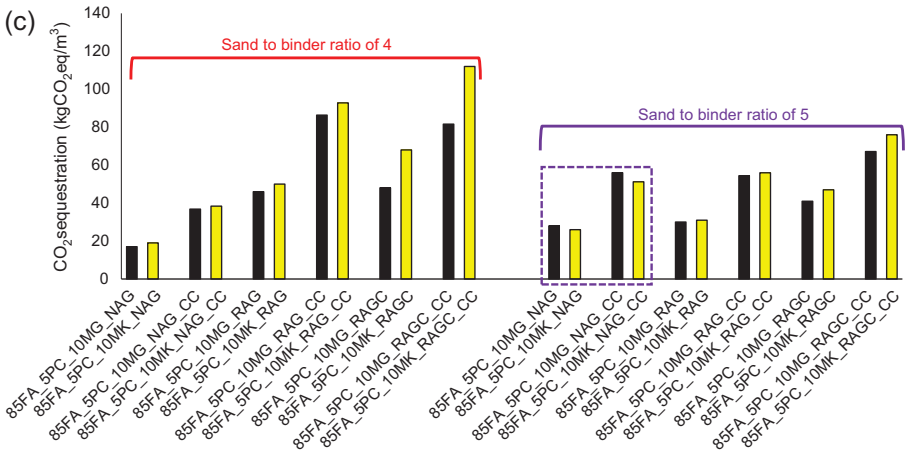

Figure 13.13 cont'd.

Table 13.4 Global warming potential of each component of mixture ($kgCO_2eq$)

Normal sand	Recycled aggregates	MG	CH	Fly ash	Water	PC	MK	SH
0.0024	0.00401	0.00526	0.416	0.00526	0.000155	0.931	0.0924	2.24

MPa, for the mixtures 80FA_10CH_10MG_RAG_CC and 80FA_10CH_10MG_RAG, respectively. It shows that using flow-through CO_2 curing resulted in reducing around 6 times the amount of carbon dioxide released into the atmosphere per 1 MPa (see Fig. 13.16(b)). Regardless of the curing method, using recycled carbonated aggregate in the mixtures with sand to binder ratio 4 led to minimum amount of carbon dioxide released into the atmosphere per 1 MPa, so that the minimum value achieved was about 6 $kgCO_2eq/m^3MPa$ in the mixture 80FA_10CH_10MK_RAGC_CC.

By increasing the sand to binder ratio from 4 to 5, generally, using flow-through CO_2 curing reduced the normalized carbon footprint to the compressive strength of the mixtures, as compared to the normalized carbon footprint to the compressive strength of the mixtures cured at ambient temperature (see Fig. 13.17). In general, regardless the curing method, using recycled aggregate and recycled carbonated aggregate reduced the amount of carbon dioxide released into the atmosphere per 1 MPa, when compared to the mixtures containing normal sand. The minimum amount of

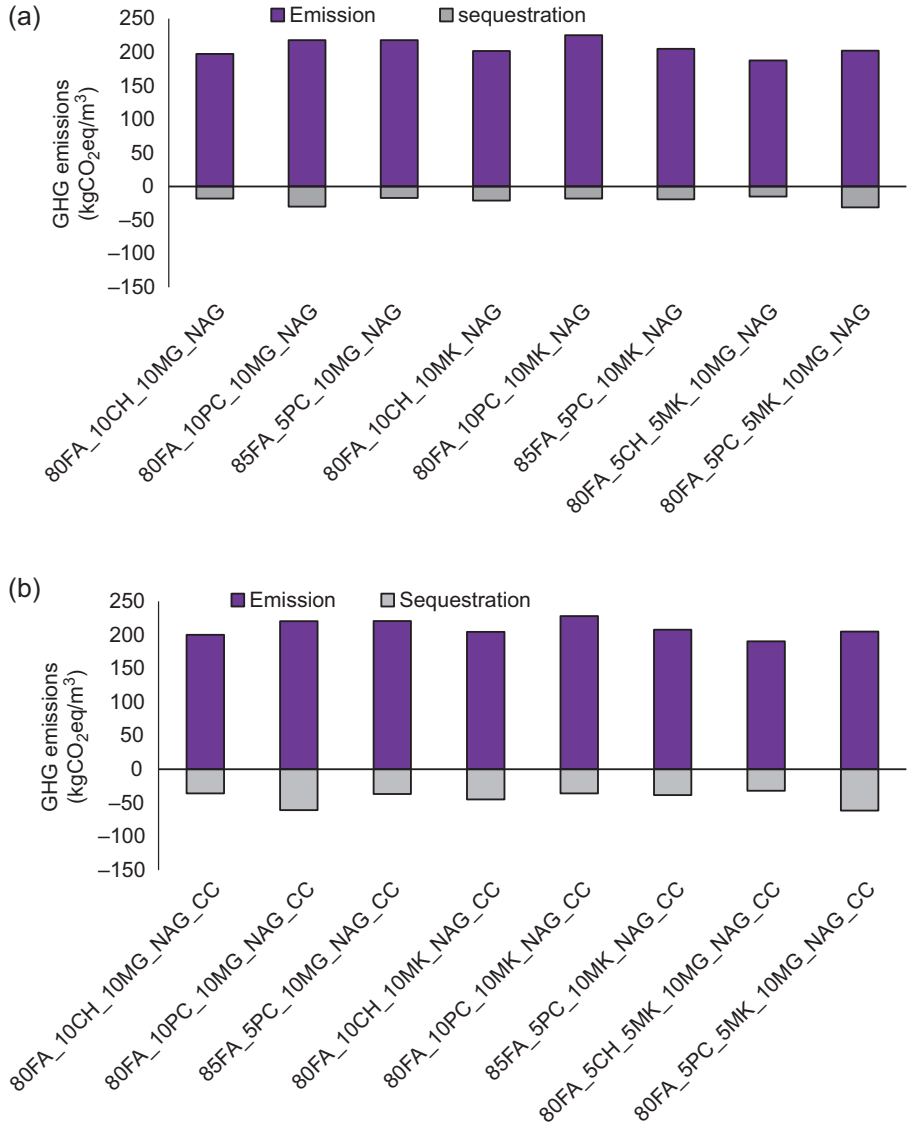

Figure 13.14 Greenhouse gas emissions for different mixtures containing sand to binder ratio 4 and: (a) normal aggregate, cured at ambient temperature; (b) normal aggregate, cured at carbonation chamber; (c) recycled aggregate, cured at ambient temperature; (d) recycled aggregate, cured at carbonation chamber; (e) recycled carbonated aggregate, cured at ambient temperature; (f) recycled carbonated aggregate cured at carbonation chamber.

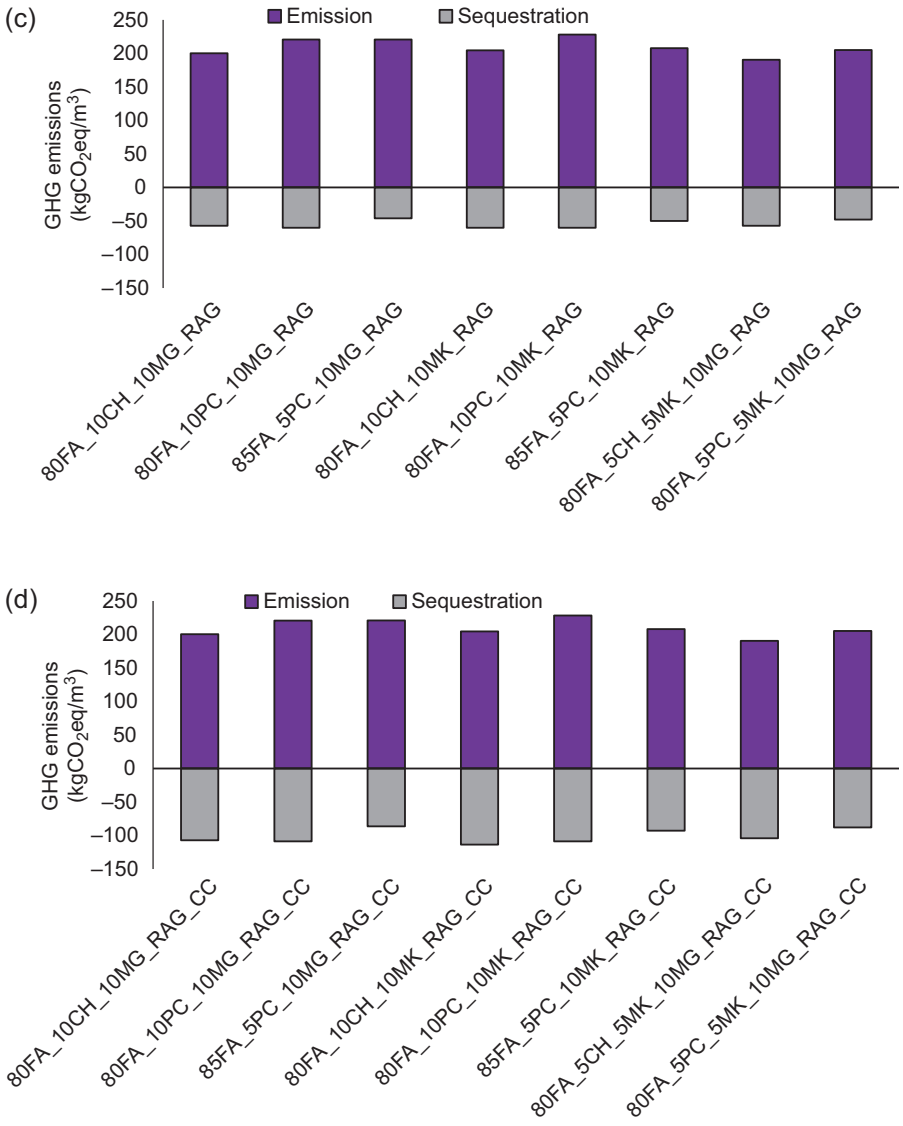

Figure 13.14 cont'd.

carbon dioxide released into the atmosphere per 1 MPa for the mixtures containing recycled aggregate and recycled carbonated aggregate were recorded as 10.3 and 10.1 $kgCO_2eq/m^3$ for the mixtures 80FA_5PC_5MK_10MG_RAG_CC and 80FA_10CH_10MG_RAGC_CC, respectively.

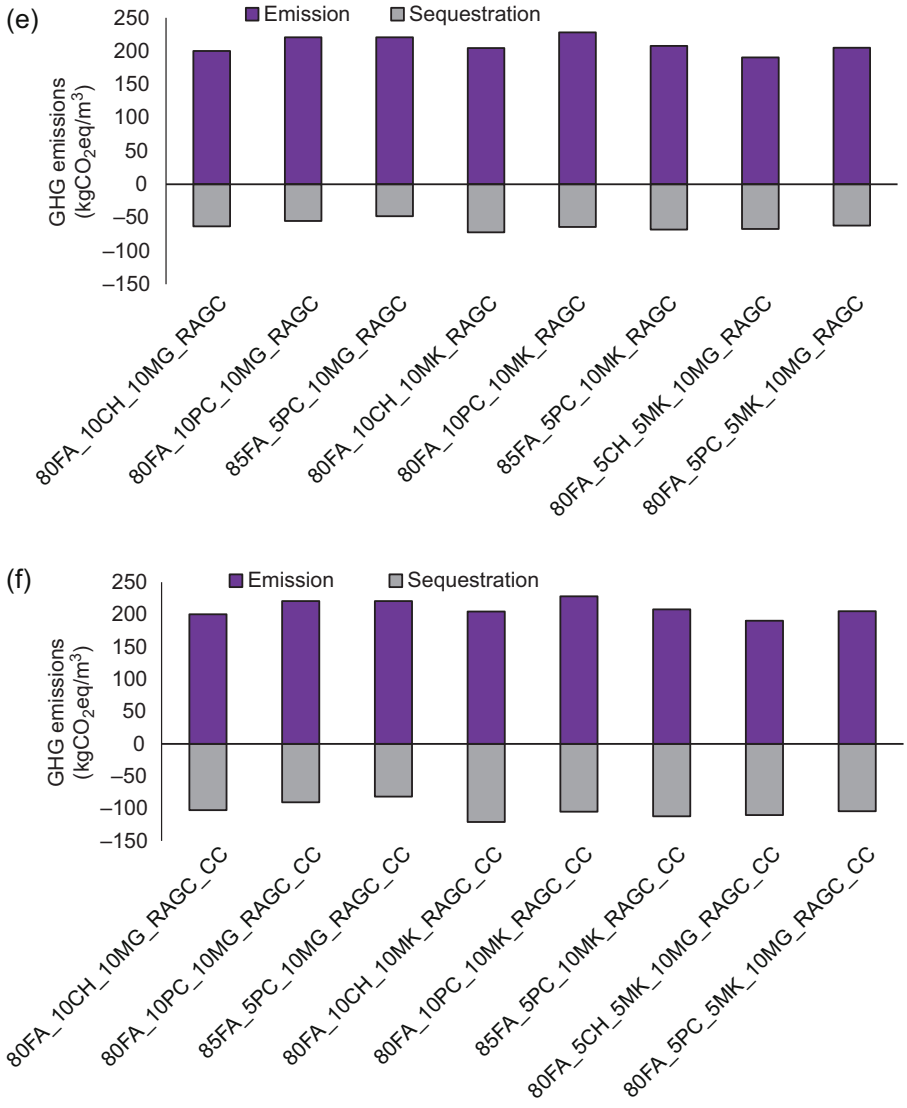

Figure 13.14 cont'd.

13.3.6 Cost analysis

The cost of mixtures for one cubic meter was calculated with respect to the prices of each of the mixture's ingredients in Table 13.5, based on data provided by their suppliers. Figs. 13.18 and 13.19 indicate the results obtained for the total price of the mixtures. Moreover, two scenarios were also assumed to consider the carbon tax in the total price of each mixture, including (1) 0.0347 Euro/kg for the carbon footprint

of the first scenario (Stanford Report, 2015); (2) 0.206 Euro/kg for the carbon footprint of mixtures of the second scenario (Moore and Diaz, 2015). The carbon tax is a complex issue; it has political and sociological implications the discussion of which are out of the scope of this study. Figs. 13.18 and 13.19 indicate the results obtained

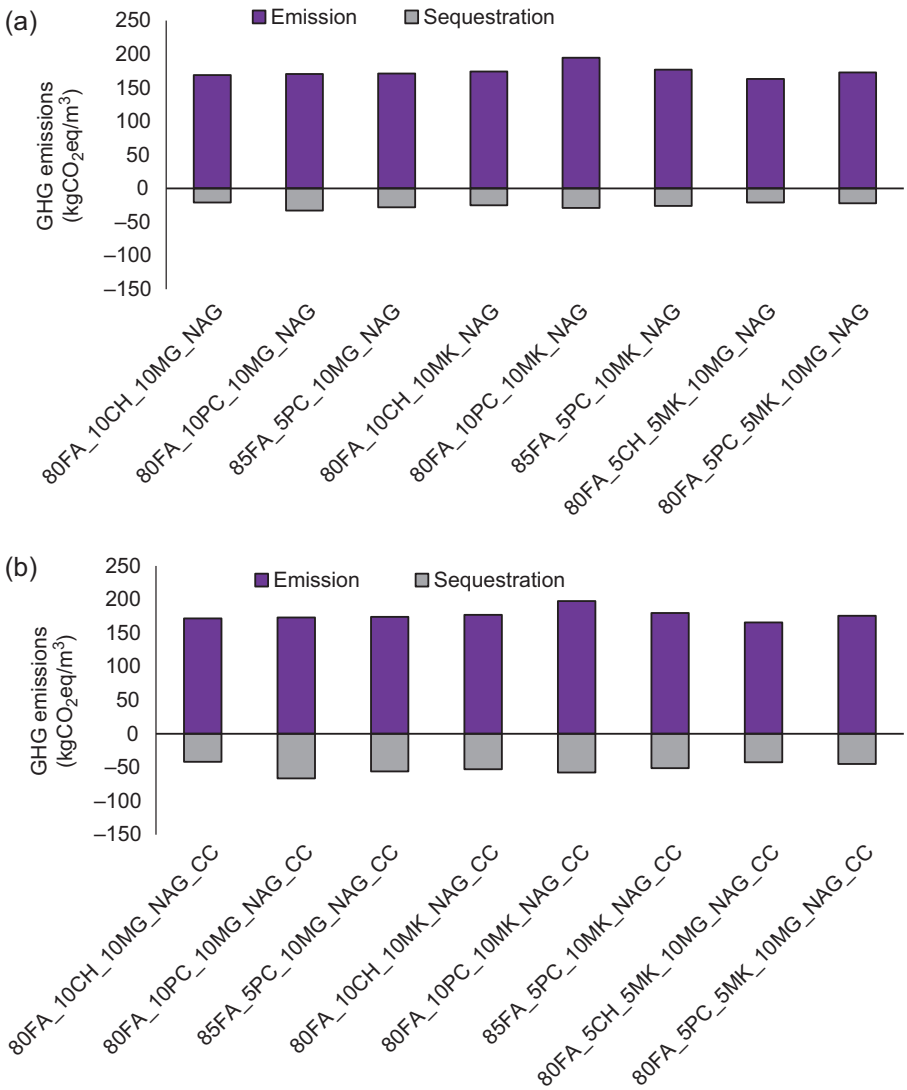

Figure 13.15 Greenhouse gas emissions for different mixtures containing sand to binder ratio 5 and: (a) normal aggregate,cured at ambient temperature; (b) normal aggregate,cured at carbonation chamber; (c) recycled aggregate,cured at ambient temperature; (d) recycled aggregate,cured at carbonation chamber; (e) recycled carbonated aggregate, cured at ambient temperature; (f) recycled carbonated aggregate, cured at carbonation chamber.

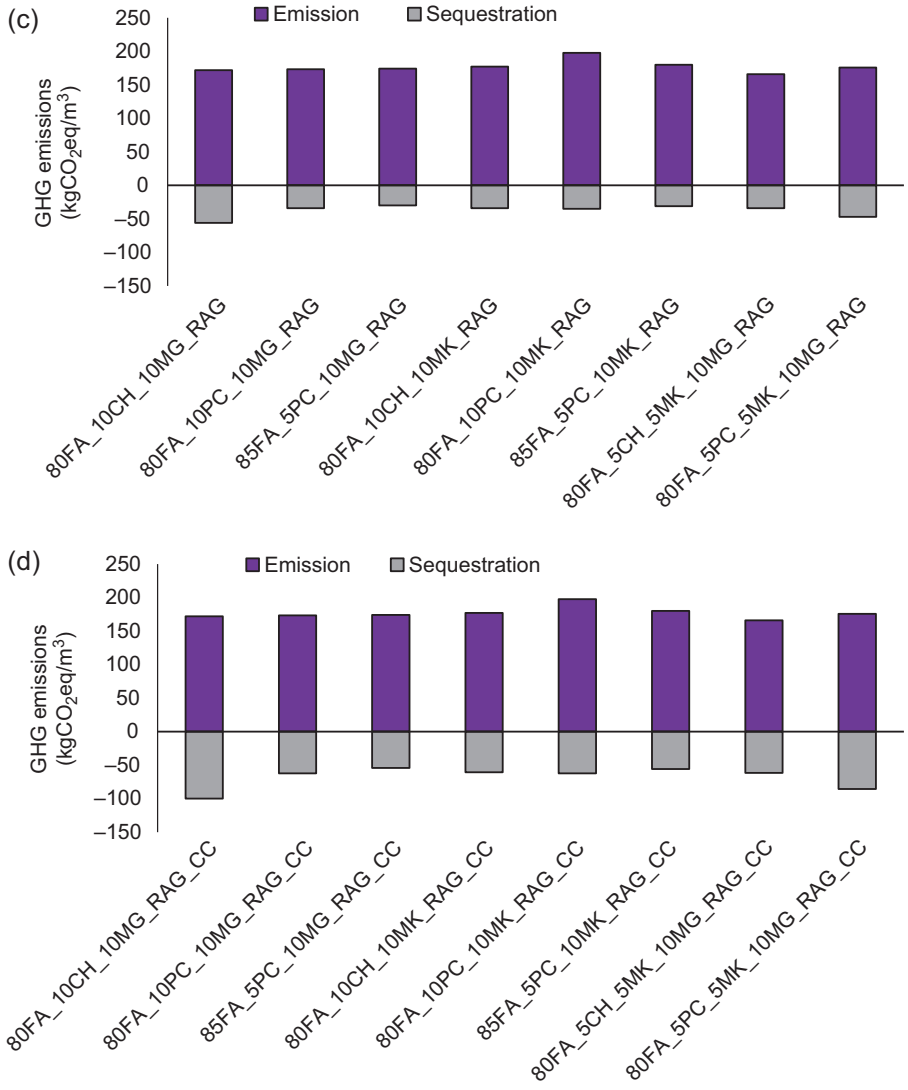

Figure 13.15 cont'd.

for the total price of the mixtures. Regardless of the carbon tax defined in those two scenarios, the minimum and maximum cost of the mixtures with sand to binder ratio 4 and normal sand were detected in the mixtures 80FA_10PC_10MG_NAG_CC and 80FA_10CH_10MK_NAG, respectively (see Fig. 13.18(a) and (b)). Regarding the results obtained, the material cost of the mixtures without any scenarios varied in

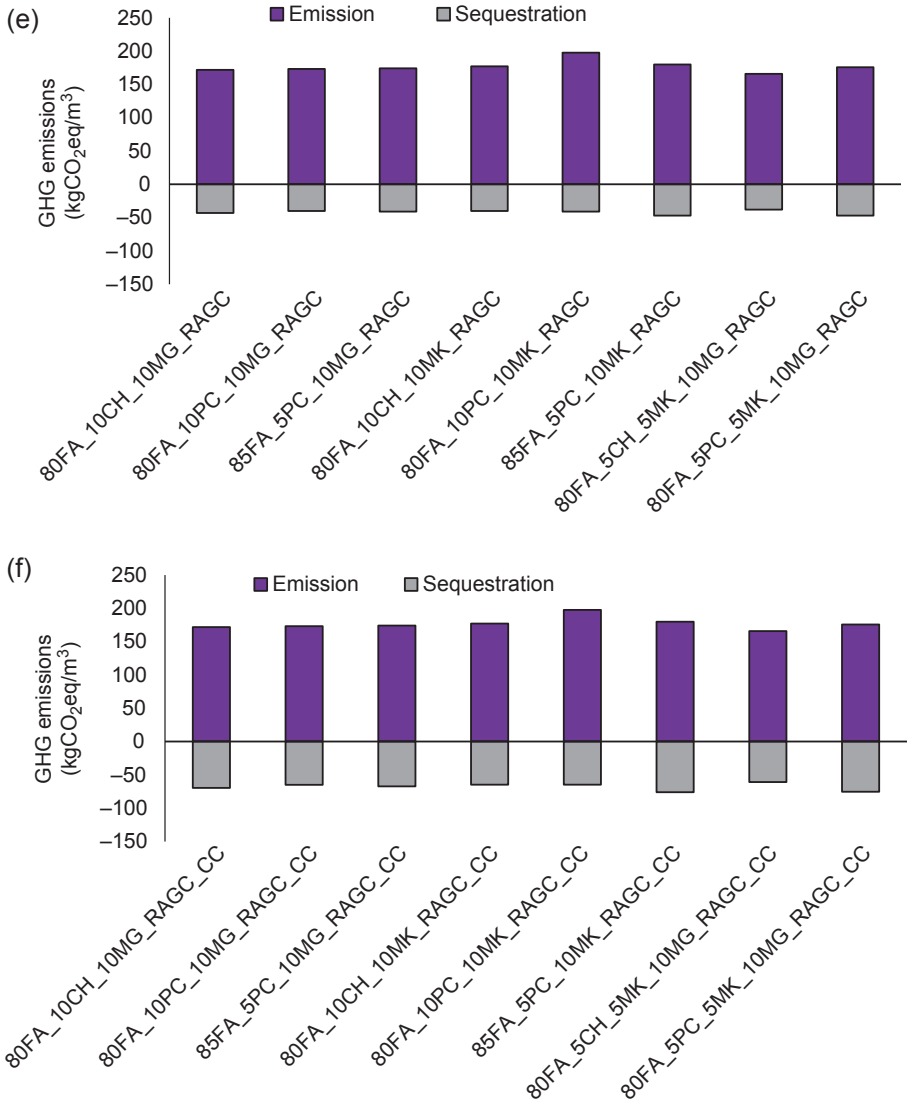

Figure 13.15 cont'd.

the range of 130 (80FA_10PC_10MG_NAG) to 150 (80FA_10CH_10MK_NAG) Euro/m^3. Replacing cement by calcium hydroxide increased the material costs (around 7%) as well as using MK instead of milled glass increased the price of the mixtures (averagely 10%). Moreover, it was observed that the effect of replacing MK by milled glass on increasing the material cost was slightly higher than replacing

calcium hydroxide by cement (about 3%). The cost of the mixtures containing sand to binder ratio 4 and normal sand varied in the range of 135−160 Euro/m^3 for the first scenario and 160−190 Euro/m^3 for the second scenario. Defining the carbon tax increased the costs of the mixtures 3%−6% for the first scenario and 23%−26% for the second scenario. Generally, replacing normal sand by recycled aggregates and including the carbon tax increased the price of the mixtures. The cost of the

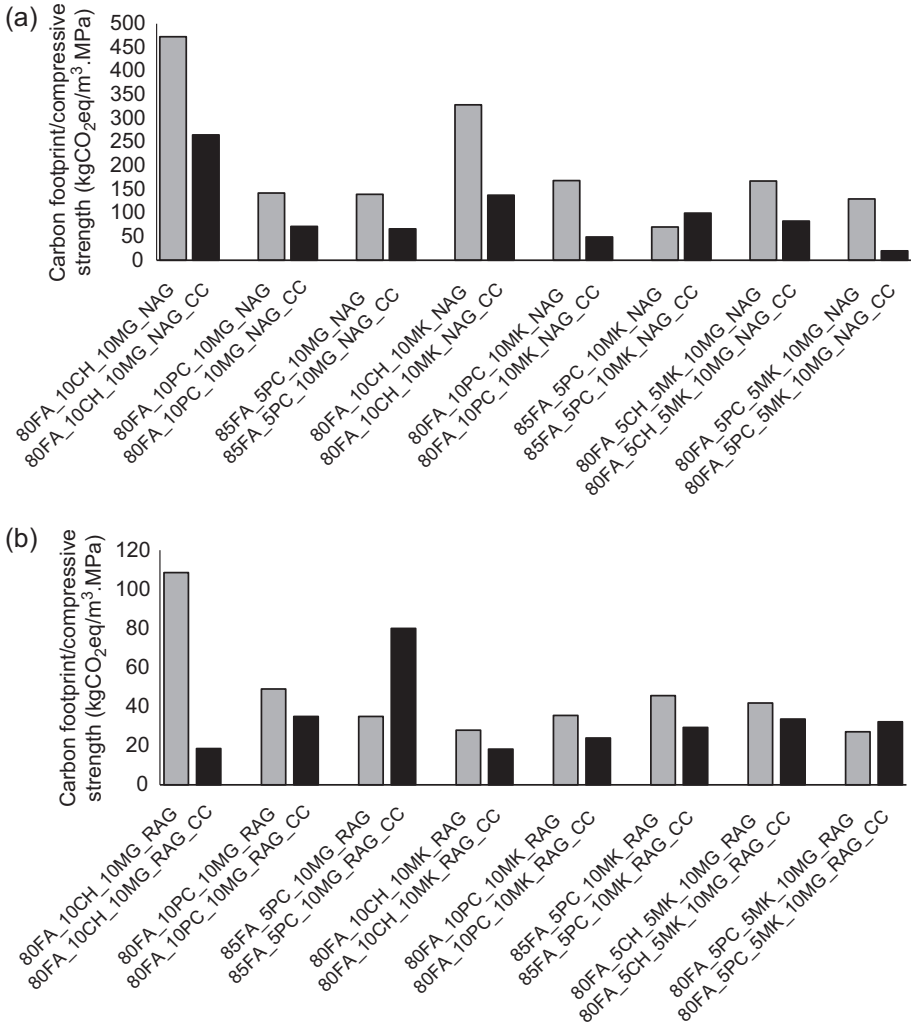

Figure 13.16 Carbon footprint to the compressive strength ratio of different mixtures containing sand to binder ratio 4 : (a) normal aggregate; (b) recycled aggregate; (c) recycled carbonated aggregate.

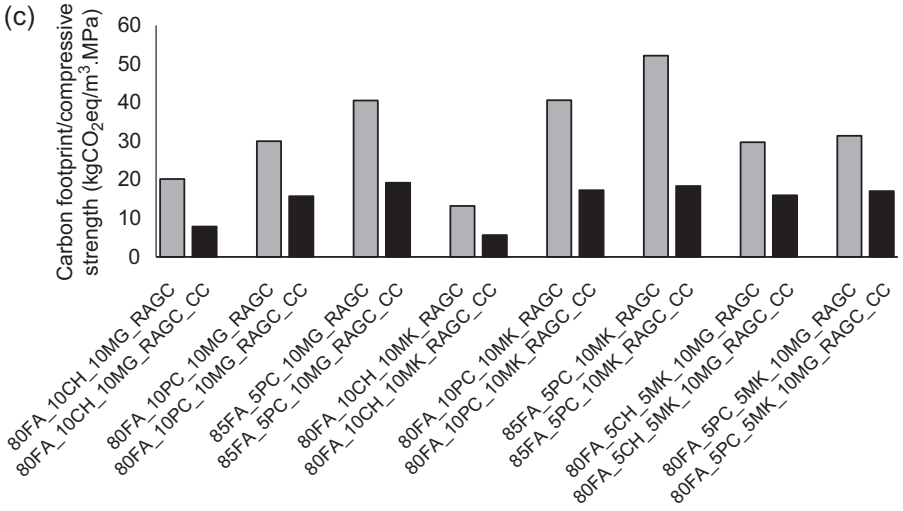

Figure 13.16 cont'd.

mixtures containing sand to binder ratio 4 and recycled aggregate without any scenarios varied in the range of 175 (80FA_10PC_10MG_RAG) to 195 (80FA_10CH_10MK_RAG) Euro/m^3. Replacing recycled aggregate by normal sand increased the material costs in the range of 30%−35%. Furthermore, it was detected that the total cost of the mixtures varied in the range of 180 (80FA_10PC_10MG_RAG_CC) to 200 (80FA_10CH_10MK_RAG) Euro/m^3 for the first scenario and 200−225 Euro/m^3 for the second scenario. Imposing the carbon tax increased the total cost of the materials about 2% and 15% for the first and second scenarios, respectively. The minimum and maximum cost of the mixtures with sand to binder ratio 4 and recycled carbonated aggregate were found to be about 174 and 196 Euro/m^3 in the mixtures 80FA_10PC_10MG_RAGC_CC and 80FA_10CH_10MK_RAGC, respectively (see Fig. 13.18(e) and (f)). Regardless of the sand type, using flow-through CO_2 curing reduces the total cost of the mixtures because this method reduced the carbon footprint in the mixtures, as compared to the carbon footprint in the specimens cured at ambient temperature. Therefore, the total price of the mixtures cured through flow-through CO_2 gas was lower than the total price of the mixtures cured at ambient temperature. Increasing the sand to binder ratio from 4 to 5 decreased the total price of the mixtures. The material cost of the mixtures containing sand to binder ratio 5 and normal sand varied in the range of 110 (80FA_10PC_10MG_NAG) to 135 (80FA_10CH_10MK_NAG) Euro/m^3. Comparing the material costs of the mixtures containing normal sand to binder ratios of 4 and 5 revealed that increasing the sand content decreased the material cost in the range of 8%−15%. Since the cost of the mixtures containing normal sand varied in the range of 110 (80FA_10PC_10MG_NAG_CC) to 140 (80FA_10CH_10MK_NAG) Euro/m^3 for the first scenario and

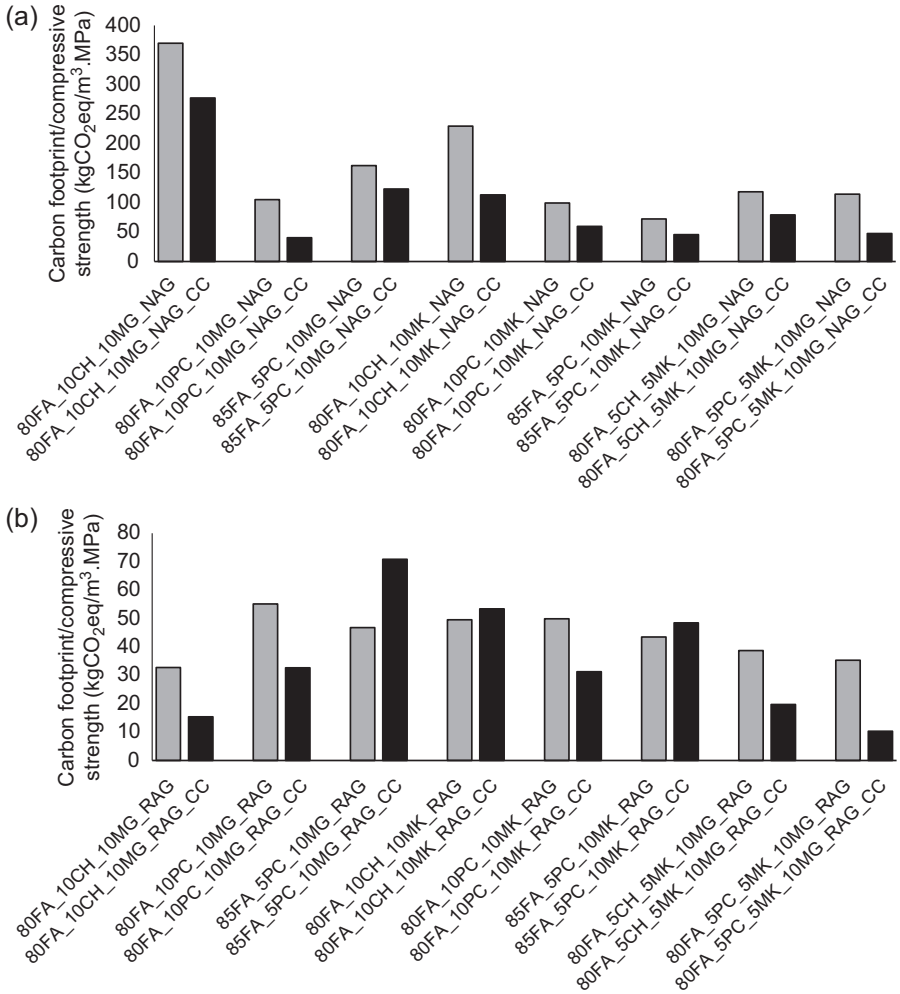

Figure 13.17 Carbon footprint to the compressive strength ratio of different mixtures containing sand to binder ratio 5 : (a) normal aggregate; (b) recycled aggregate; (c) recycled carbonated aggregate.

130 to 165 Euro/m^3 for the second scenario (Fig. 13.19(a) and (b)). Considering the carbon tax increased the total cost of the materials in the range of 1.1%−3% for the first scenario and 18%−22% for the second scenario. Regardless of the sand type and content, the maximum material cost in the mixtures was detected in the binder materials as 80% FA, 10% calcium hydroxide, and 10% MK; this fact could be derived from using simultaneously both calcium hydroxide and MK. In this study, the competitive mixture costs were observed in the mixtures that used normal sand to binder ratio 5, cured by a flow-through CO_2 gas, and used both milled glass and cement. Increasing sand content, using ambient curing conditions, the addition of calcium hydroxide and

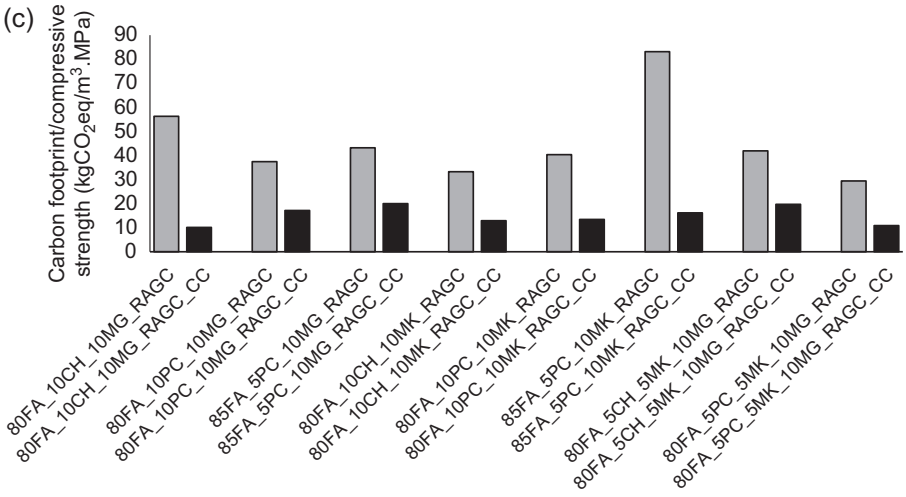

Figure 13.17 cont'd.

Table 13.5 Costs of the materials (Euro/kg)

Normal sand	Recycled aggregates	Waste glass	Calcium hydroxide	Fly ash	Water	Portland cement	Metakaolin	SH
0.020	0.047	0.009	0.283	0.03	0.01	0.1	0.29	0.85

MK increases the total mixture cost. Like the mixtures with sand to binder ratio 4, using recycled aggregate instead of normal sand increased the cost of the mixtures due to the higher cost of recycled aggregates in comparison to normal sand. The material cost of the mixtures containing sand to binder ratio 5 and recycled carbonated aggregates varied in the range of 160 (80FA_10PC_10MG_RAGC) to 185 (80FA_10CH_10MK_RAGC) Euro/m^3. Additionally, comparing the material costs of the mixtures containing recycled aggregate to binder ratios of 4 and 5 revealed that increasing recycled aggregate content decreased the material cost in the range of 6%−10%. The minimum and maximum cost of the mixtures with sand to binder ratio 5 and recycled aggregate were observed in the mixture 80FA_10PC_10MG_RAG_CC (160 Euro/m^3, the first scenario) and 80FA_10CH_10MK_RAG (190 Euro/m^3, the second scenario), respectively (see Figs. 13.19(c) and 13.16(d)). The cost of the mixtures with recycled carbonated aggregate varied in the range of 160 (for 80FA_10PC_10MG_RAGC_CC) to 190 (for 80FA_10CH_10MK_RAGC) Euro/m^3 for the first scenario and 180 to 215 Euro/m^3 for the second scenario. Therefore, regarding the results, it could be concluded that the carbon tax increased the total cost of the materials in the range of 1%−2% for the first scenario and 12%−16% for the second scenario.

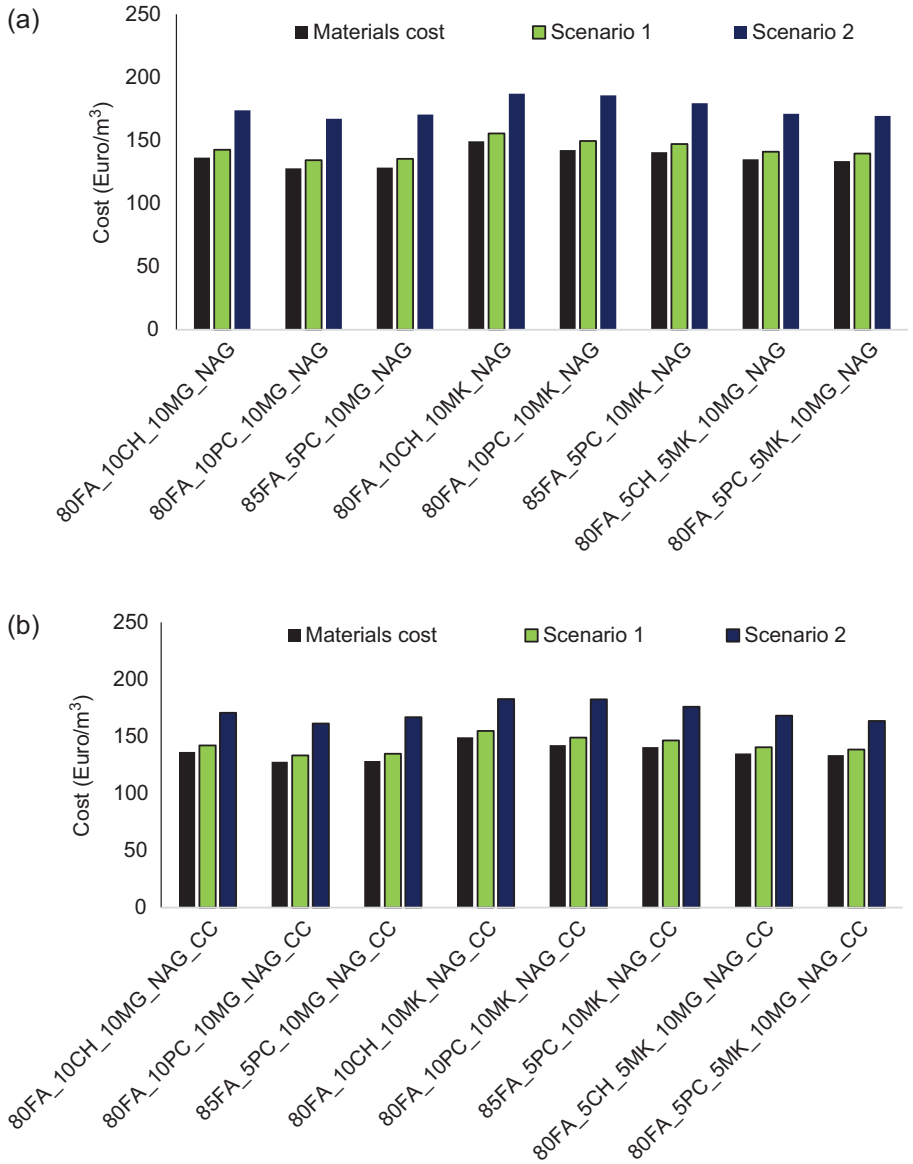

Figure 13.18 Total cost of the mixtures containing sand to binder ratio 4 : (a) normal aggregate, cured at ambient temperature; (b) normal aggregate,cured at carbonation chamber; (c) recycled aggregate,cured at ambient temperature; (d) recycled aggregate, cured at carbonation chamber; (e) recycled carbonated aggregate, cured at ambient temperature; (f) recycled carbonated aggregate, cured at carbonation chamber.

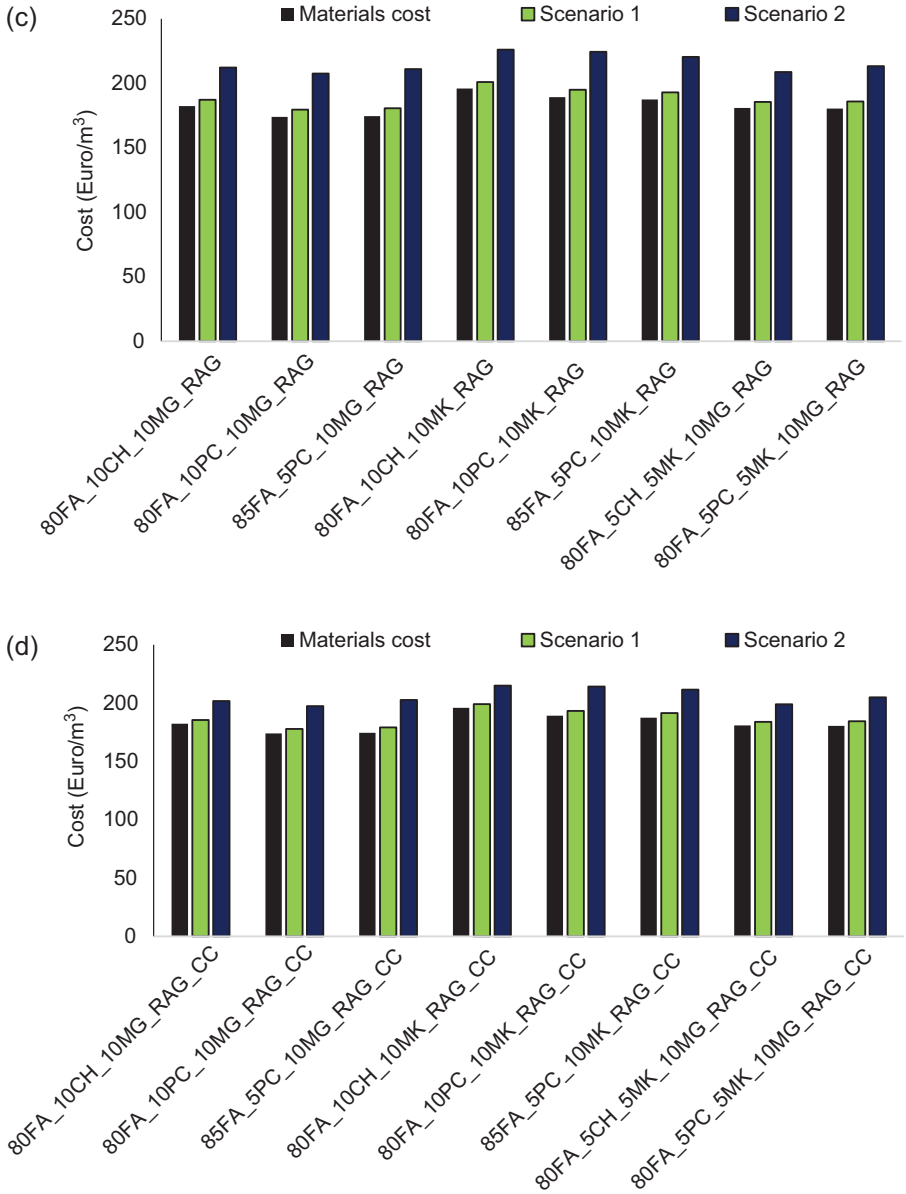

Figure 13.18 cont'd.

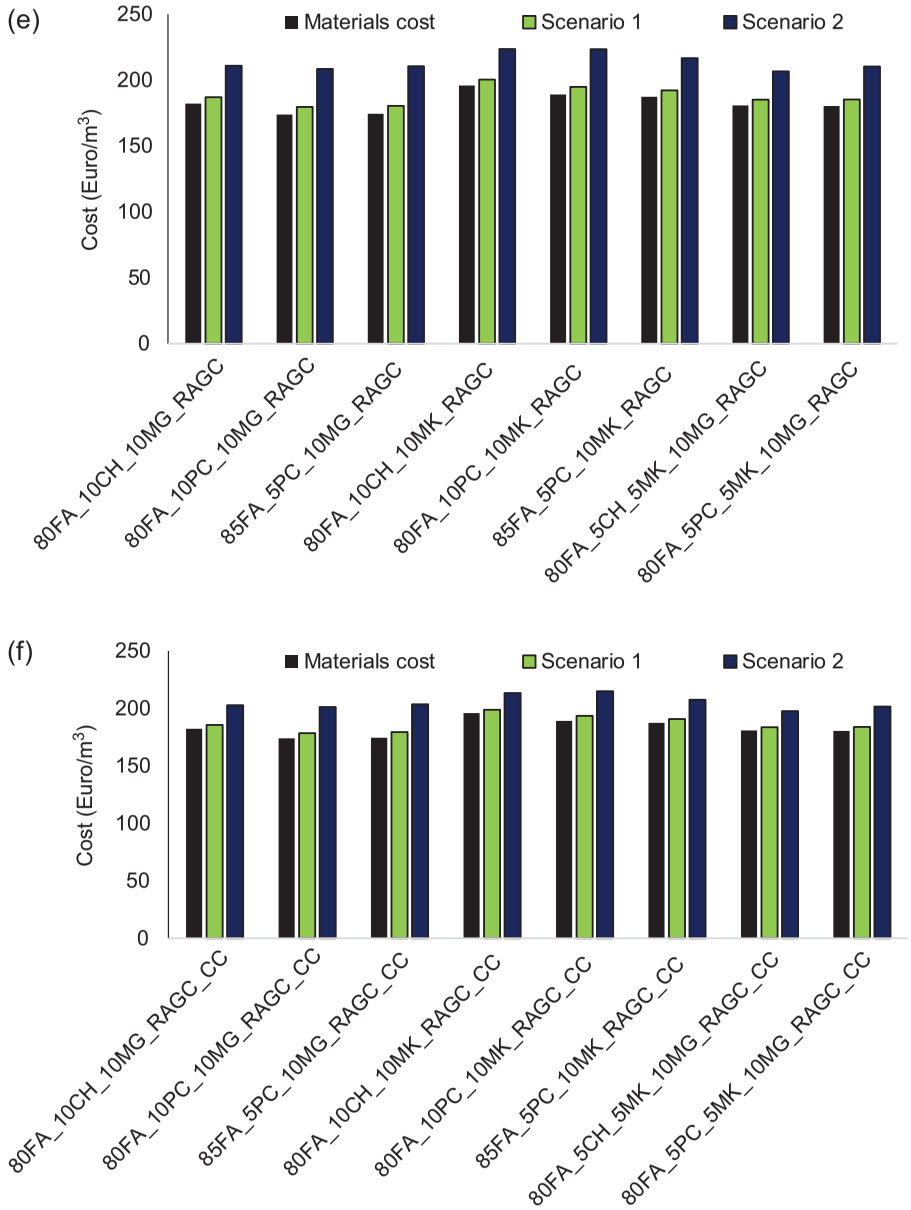

Figure 13.18 cont'd.

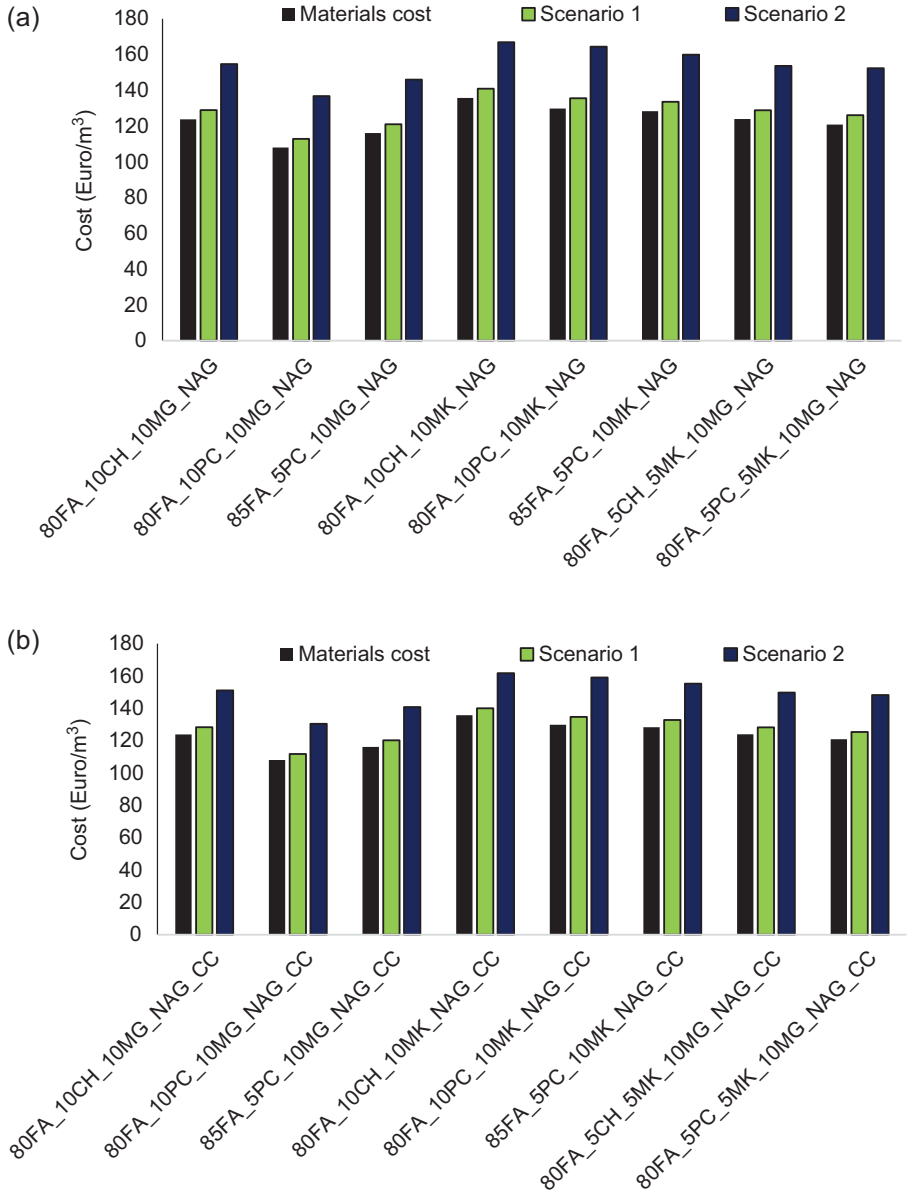

Figure 13.19 Total cost of the mixtures containing sand to binder ratio 5 : (a) normal aggregate, cured at ambient temperature; (b) normal aggregate, cured at carbonation chamber; (c) recycled aggregate, cured at ambient temperature; (d) recycled aggregate, cured at carbonation chamber; (e) recycled carbonated aggregate cured at ambient temperature; (f) recycled carbonated aggregate, cured at carbonation chamber.

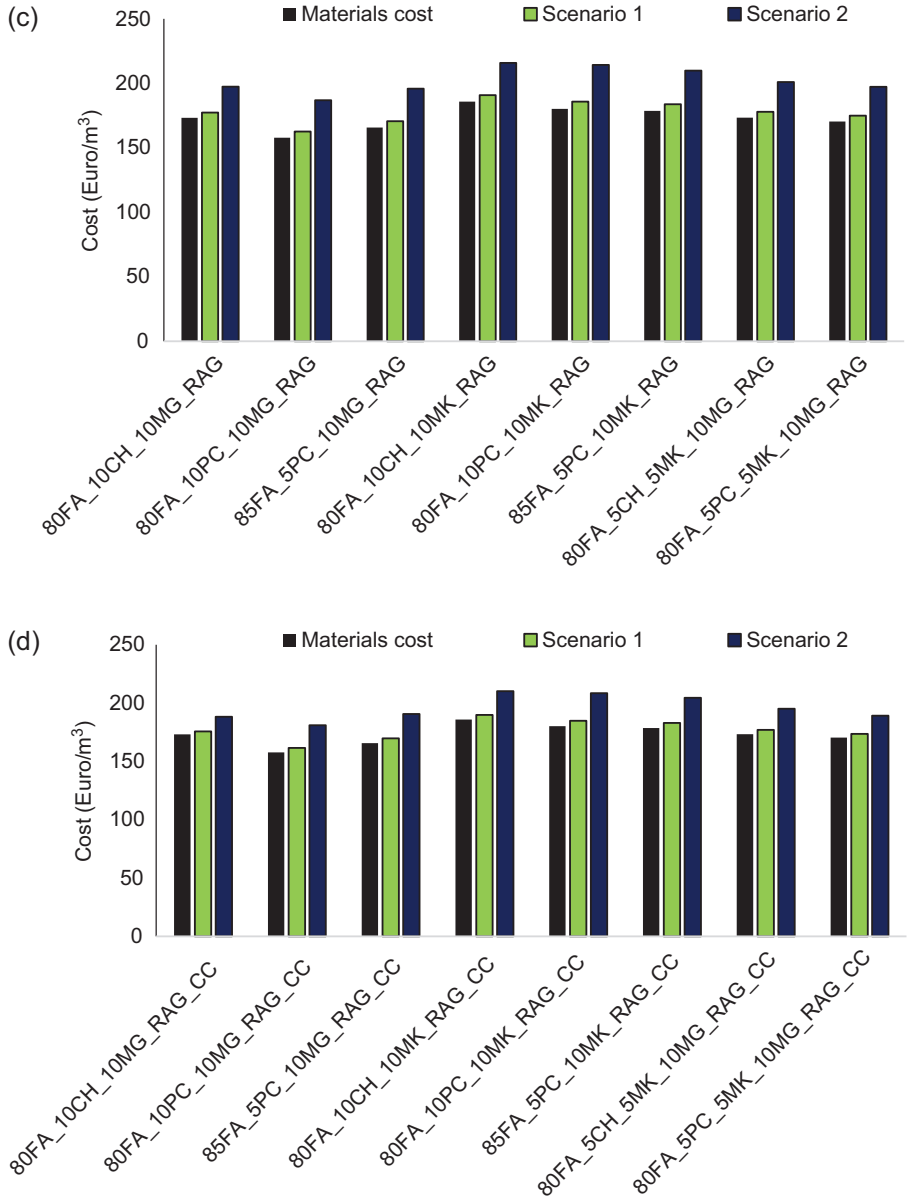

Figure 13.19 cont'd.

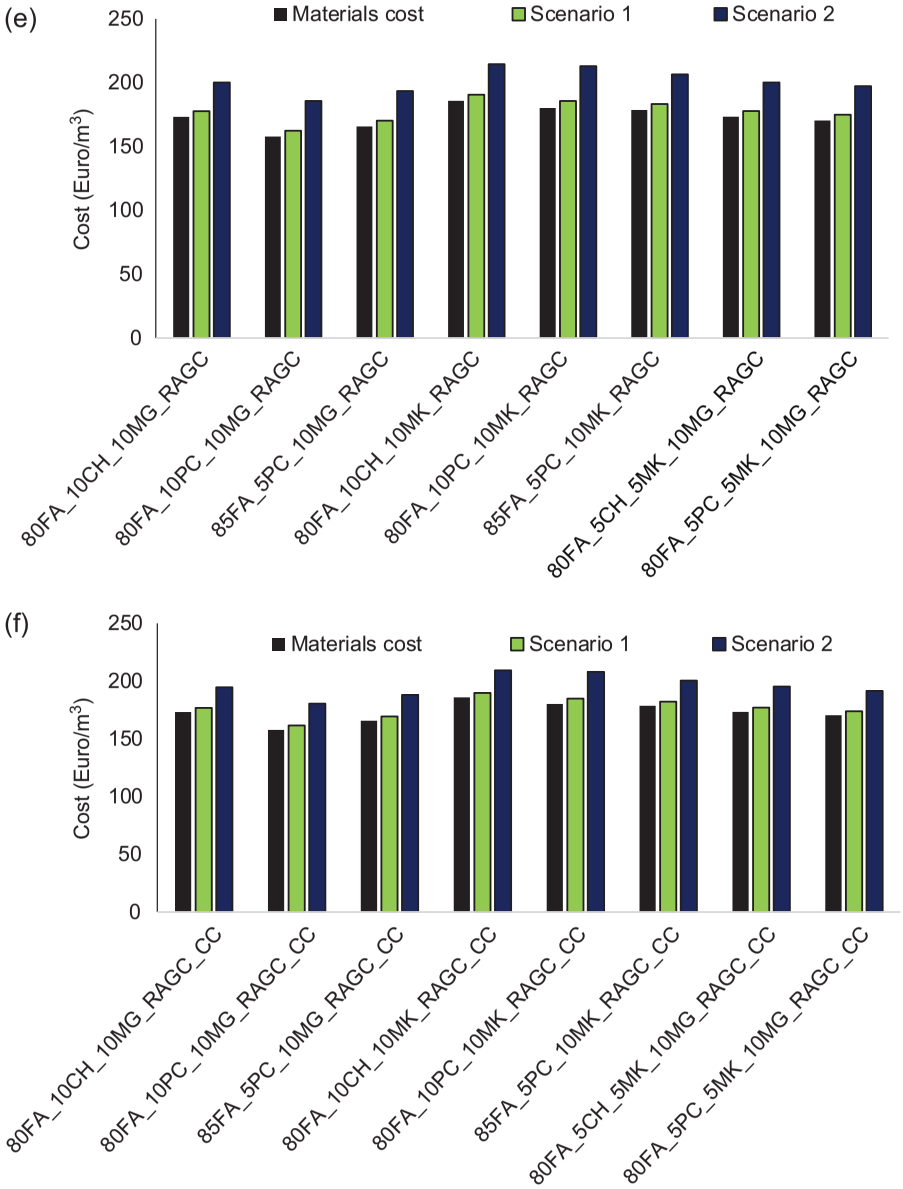

Figure 13.19 cont'd.

13.4 Conclusions

Considering the results of the study, the following conclusions were reached:

1. Using accelerated CO_2 curing method increased the compressive strength of FA alkaline-based mortars containing the normal aggregate, as compared to curing at the ambient temperature.
2. Regardless of the duration of curing and the ratio of sand to binder, using simultaneously recycled carbonated aggregate and accelerated CO_2 curing significantly increased the compressive strength of the mixtures.
3. Generally, increasing the sand binder ratio from 4 to 5 reduced the compressive strength.
4. For mixtures cured at the ambient temperature, the maximum compressive strength was about 10 MPa for the mixture 80FA_10CH_10MK_RAGC. Using accelerated CO_2 curing led to a maximum compressive strength of about 15 MPa for the mixture 80FA_10CH_10MK_RAGC_CC.
5. Regardless of the sand to binder ratio, the maximum increase of the compressive strength due to use of accelerated CO_2 curing method instead of the ambient temperature was measured for the mixture 80FA_10CH_10MG_RAGC, so that these increases were 9 and 5.5 times for the sand to binder ratios of 4 and 5, respectively.
6. It was observed that the sand had the greatest impact on increasing or decreasing trend of the CO_2 sequestration. Moreover, regardless of the raw materials and sand to binder ratio, it was noticed that using recycled aggregate and recycled carbonated aggregate generally led to obtain the maximum CO_2 sequestration in the mixtures.
7. It was found that using accelerated CO_2 curing significantly increases the CO_2 sequestration, as compared to the CO_2 sequestration cured at the lab temperature, so that the maximum effect of using a flow-through CO_2 curing on increasing the CO_2 sequestration was found in the mixtures containing normal sand and a sand to binder ratio 4 (85FA_5PC_10MG_NAG_CC more than 2 times, as compared to 85FA_5PC_10MG_NAG).
8. Considering the results, the minimum and maximum CO_2 sequestration were detected in the mixtures of 80FA_5CH_5MK_10MG_NAG (15 $kgCO_2eq/m^3$) and 80FA_10CH_10MK_RAGC_CC (121 $kgCO_2eq/m^3$) with sand to binder ratio 4, respectively.

Acknowledgment

The authors would like to acknowledge the financial support of the Foundation for Science and Technology (FCT) in the frame of project IF/00706/2014-UM.2.15.

References

Abdollahnejad, Z., Miraldo, S., Pacheco-Torgal, F., Barroso Aguiar, J., 2016. Cost-efficient one-part alkali-activated mortars with low global warming potential for floor heating systems applications. European Journal of Environmental and Civil Engineering 21, 412–429.

American Coal Ash Association, 2016. https://www.acaa-usa.org/Publications/Production-Use-Reports.

Ashraf, W., Olek, J., 2016. Carbonation behavior of hydraulic and non-hydraulic calcium silicates: potential of utilizing low-lime calcium silicates in cement-based materials. Journal of Materials Science 51 (13), 6173–6191.

Bernal, S., 2014. Resistance to carbonation of alkali-activated materials. In: Pacheco-Torgal, F., Labrincha, J.A., Leonelli, C., Palomo, A., Chindaprasirt, P. (Eds.), Handbook of Alkali-activated Cements, Mortars and Concretes. WoodHead Publishing Limited- Elsevier Science and Technology, Abington Hall, Cambridge, UK, pp. 319−332.

Bernal, S., Rodríguez, E., Kirchheim, A., Provis, J., 2016. Management and valorisation of wastes through use in producing alkali-activated. Cement materials. Journal of Chemical Technology & Biotechnology. https://doi.org/10.1002/jctb.4927.

Bertos, M.F., Simons, S.J.R., Hills, C.D., Carey, P.J., 2004. A review of accelerated carbonation technology in the treatment of cement-based materials and sequestration of CO_2. Journal of Hazardous Materials 112 (3), 193−205.

El-Hassan, H., Shao, Y., 2014. Carbon storage through concrete block carbonation. Journal of Clean Energy Technology 2, 287−291.

El-Hassan, H., Shao, Y., 2015. Early carbonation curing of concrete masonry units with Portland limestone cement. Cement and Concrete Composites 62, 168−177.

Galan, I., Andrade, C., Mora, P., Sanjuan, M., 2010. Sequestration of CO_2 by concrete carbonation. Environmental Science and Technology 44, 3181−3186.

Garcia-Lodeiro, I., Donatello, S., Fernandez-Jimenez, A., Palomo, A., 2016. Hydration of hybrid alkaline cement containing a very large proportion of fly ash: a descriptive model. Materials 9, 605.

Han, Y.S., et al., 2005. Effect of flow rate and CO_2 content on the phase and morphology of $CaCO_3$ prepared by bubbling method. Journal of Crystal Growth 276 (3), 541−548.

Hansen, J., Sato, M., Kharecha, P., von Schuckmann, K., Beerling, D.J., Cao, J., Marcott, S., Masson-Delmotte, V., Prather, M.J., Rohling, E.J., Shakun, J., Smith, P., 2017. Young people's burden: requirement of negative CO_2 emissions. Earth System Dynamics. https://doi.org/10.5194/esd-2016-42.

He, P., Shi, C., Tu, Z., Poon, C.S., Zhang, J., 2016. Effect of further water curing on compressive strength and microstructure of CO_2-cured concrete. Cement and Concrete Composites 72, 80−88.

Jang, J.G., Lee, H.K., 2016. Microstructural densification and CO_2 uptake promoted by the carbonation curing of belite-rich Portland cement. Cement and Concrete Research 82, 50−57.

Jang, J.G., Kim, G.M., Kim, H.J., Lee, H.K., 2016. Review on recent advances in CO_2 utilization and sequestration technologies in cement-based materials. Construction and Building Materials 127, 762−773.

Kwasny, J., Basheer, P.A.A., Russell, M.I., 2014. CO_2 sequestration in cement-based materials during mixing process using carbonated water and gaseous CO_2. In: 4th International Conference on the Durability of Concrete Structures, 24−26 July. Purdue University, West Lafayette.

Larrard, F., Belloc, A., 1997. The influence of aggregate on the compressive strength of normal and high-strength concrete. ACI Materials 94, 417−426.

Liu, S., Dou, Z., Zhang, S., Zhang, H., Guan, X., Feng, C., Zhang, J., 2017. Effect of sodium hydroxide on the carbonation behavior of β-dicalcium silicate. Construction and Building Materials 150, 591−594.

Martinez-Lopez, R., Escalante-Garcia, E., 2016. Alkali activated composite binders of waste silica soda lime glass and blast furnace slag: strength as a function of the composition. Construction and Building Materials 119 (30), 119−129. https://doi.org/10.1016/j.conbuildmat.2016.05.064.

Moore, F., Diaz, D., 2015. Temperature impacts on economic growth warrant stringent mitigation policy. Nature Climate Change 5, 127−131.

Mote, C., Dowling, J., Zhou, J., 2016. The power of an idea: the international impacts of the grand challenges for engineering. Engineering 2, 4−7.

Ouellet-Plamondon, C., Habert, G., 2014. Life cycle analysis (LCA) of alkali-activated cements and concretes. In: Pacheco-Torgal, F., Labrincha, J., Palomo, A., Leonelli, C., Chindaprasirt, P. (Eds.), Handbook of Alkali-activated Cements, Mortars and Concretes. WoodHead Publishing-Elsevier, Cambridge, pp. 663−686.

Pacheco-Torgal, F., Abdollahnejad, Z., Miraldo, S., Kheradmand, M., 2016. Alkali-activated cement-based binders (AACB) as durable and cost competitive low CO2 binders: some shortcomings that need to be addressed. In: Nazari, Sanjayan (Eds.), Handbook of Low Carbon Concrete. Elsevier Science and Tech, Waltham, US, pp. 1−15. https://doi.org/10.1016/B978-0-12-804524-4.00009-9.

Payá, J., Monzó, J., Borrachero, M.V., Tashima, M.M., 2014. Reuse of aluminosilicate industrial waste materials in the production of alkali-activated concrete binders. In: Pacheco-Torgal, F., Labrincha, J., Palomo, A., Leonelli, C., Chindaprasirt, P. (Eds.), Handbook of Alkali-activated Cements, Mortars and Concretes. WoddHead Publishing, Cambridge, UK, pp. 487−518. https://doi.org/10.1533/9781782422884.4.487.

Peter, M.A., Muntean, M., Meier, S.A., Böhm, M., 2008. Competition of several carbonation reactions in concrete: a parametric study. Cement and Concrete Research 38, 1385−1393.

Provis, J.L., 2014. Geopolymers and other alkali activated materials: why, how, and what? Materials and Structures 47, 11−25. https://doi.org/10.1617/s11527-013-0211-5.

Redden, R., Neithalath, N., 2014. Microstructure, strength, and moisture stability of alkali activated glass powder-based binders. Cement and Concrete Composites 45, 46−56.

Rostami, V., Shao, Y., Boyd, A.J., 2011. Durability of concrete pipes subjected to combined steam and carbonation curing. Construction and Building Materials 25, 3345−3355.

Šavija, B., Luković, M., 2016. Carbonation of cement paste: understanding, challenges, and opportunities. Construction and Building Materials 117, 285−301.

Shao, Y., El-hassan, H., 2013. CO_2 utilization in concrete. Third International Conference Sustainable Construction Material Technology.

Stanford Report, 2015. Estimated Social Cost of Climate Change Not Accurate, Stanford Scientists Say. Retrieved from: http://news.stanford.edu/news/2015/january/emissions-social-costs-011215.

Wang, W.-C., Chen, B.-T., Wang, H.-Y., Chou, H.-C., 2016. A study of the engineering properties of alkali-activated waste glass material (AAWGM). Construction and Building Materials 112, 962−969. https://doi.org/10.1016/j.conbuildmat.2016.11.103.

Ylmen, R., Jäglid, U., 2013. Carbonation of Portland cement studied by diffuse reflection fourier transform infrared spectroscopy. International Journal of Concrete Structures and Materials 7 (2), 119−125.

Yu, P., Kirkpatrick, R.J., Poe, B., McMillan, P.F., Cong, X., 1999. Structure of calcium silicate hydrate (C-S-H): near-, mid-, and far-infrared spectroscopy. Journal of the American Ceramic Society 82, 742−748.

Zhang, Z., Huisingh, D., 2017. Carbon dioxide storage schemes: technology, assessment and development. Journal of Cleaner Production 142, 1055−1064.

Zhang, M., Wruck, B., Graeme-Barber, A., Salje, E., Carpenter, M., 1996. Phonon spectra of alkali feldspars; phase transitions and solid solutions. American Mineralogist 81 (1−2), 92−104.